Tectonophysics 807 (2021) 228797

Contents lists available at ScienceDirect

Tectonophysics

journal homepage: www.elsevier.com/locate/tecto

The influence of subsurface geology on the distribution of earthquakes during the 2016-–2017 Central Italy seismic sequence

M.R. Barchi [a], F. Carboni [a,*], M. Michele [b], M. Ercoli [a], C. Giorgetti [a], M. Porreca [a], S. Azzaro [a], L. Chiaraluce [b]

[a] Dipartimento di Fisica e Geologia, Università degli Studi di Perugia (CRUST Member, Centro interUniversitario per l'analisi SismoTettonica Tridimensionale Con Applicazioni Territoriali)
[b] Istituto Nazionale di Geofisica e Vulcanologia

ARTICLE INFO

Keywords:
Normal faults
Seismotectonics
Seismic reflection profiles
Apennines

ABSTRACT

In 2016–2017, a destructive sequence of earthquakes affected a wide portion of Central Italy, activating a complex, 80-km long system of SW-dipping normal faults and causing impressive surface faulting and widespread damage. Former studies providing reconstructions of the fault systems activated during this sequence, are mostly based on high-resolution seismological and geodetic data. In this paper, we integrate surface and subsurface geological data with the ones obtained by an irregular network of seismic reflection profiles, aimed at providing a comprehensive reconstruction of the subsurface lithologies and structures in this area. We have constructed a set of five geological cross-sections, passing through the mainshock epicentral areas (Mw > 5.5) of the seismic sequence. The cross-sections are extrapolated down to a depth of ca. 12 km, along which we have plotted relocated seismicity. Combined geological and seismological data support a new 3D seismotectonic model, illustrating the propagation through time and space of the seismic ruptures during the sequence. Our results show that the litho-mechanical stratigraphy exerted a primary control on the distribution of seismicity, as it is mostly hosted in the more competent lithologies (i.e. the Late Triassic-Paleogene succession, consisting of carbonates and evaporites). In addition, we illustrate the crucial role played by the inherited compressional structures in determining the lateral and vertical variations of the rheological properties of the upper crust and, eventually, the overall geometry and segmentation of the seismogenic extensional system. The workflow proposed here can be applied to other seismogenic zones throughout the world, since reliable seismotectonic models require an accurate reconstruction of the subsurface geological setting, based on a close integration of geological, geophysical and seismological data.

1. Introduction

Substantial improvement in the techniques of acquisition and analysis of seismological data, achieved in the last decades, provides unprecedented, detailed reconstructions of the active fault systems at seismogenic depths. High resolution in the detection and location of earthquake catalogues allows the location, dimension and attitude (strike, dip, length and width) of single fault segments to be defined. Outstanding examples come from the extensional fault systems in Central Italy, where seismological and geodetic networks have given progressively improved images of the faults activated during the Umbria-Marche (1997–1998, Chiaraluce et al., 2003), L'Aquila 2009 (Valoroso et al., 2013) and Central Italy (2016–2017, Chiaraluce et al., 2017; Improta et al., 2019; Michele et al., 2020) sequences. These reconstructions were based mainly on aftershock distributions, derived from the application and integration of both relative (e.g. double difference; Waldhauser and Ellsworth, 2000) and absolute (non-linear algorithm; Lomax et al., 2000) locations techniques.

Unfortunately, there has been little corresponding improvement in the understanding of the subsurface geology in the same region. There are high-quality, detailed geological maps (Centamore et al., 1992; Koopman, 1983; Pierantoni et al., 2013; Carta Geologica Regionale 1:10000 – Regione Marche, 2014; Carta Geologica Regionale 1:10000 – Regione Umbria, 2016; Ghisetti and Vezzani, 1986), but the connection between the Quaternary faults exposed at the surface and the active faults at seismogenic depths (6–10 km in this region) is difficult to

* Corresponding author.
E-mail address: filippocarboni@ymail.com (F. Carboni).

https://doi.org/10.1016/j.tecto.2021.228797
Received 26 October 2020; Received in revised form 16 February 2021; Accepted 18 February 2021
Available online 25 February 2021

determine, and would require the availability of specifically aimed geophysical surveys. In this region, however, no large scale geophysical acquisition and/or borehole drilling for scientific purposes has been undertaken for many years, and the most relevant information is provided by an irregular network of seismic reflection profiles, acquired by oil companies in the 1980's (e.g. Bally et al., 1986).

In Central Italy, the seismicity is related to a system of normal faults related to horizontal WSW-ENE extension, at a rate of 3–4 mm/yr derived from geodetic data at a regional scale (e.g., Pondrelli et al., 2006; D'Agostino et al., 2011; Anderlini et al., 2016; Devoti et al., 2017). In the last 20 years, a huge amount of seismological and seismotectonic studies have been performed in this region. However, the actual geometry of the seismogenic faults (e.g. listric vs. planar), the nature of the rocks involved in the deformation and how they may influence the mechanical behaviour of the active faults, and the role of the pre-existing/inherited structures (e.g. in fostering reactivation phenomena and/or promoting segmentation of the activated fault systems) are still issues of much debate and disagreement.

In 2016–2017, a damaging seismic sequence affected a wide portion of Central Italy (Fig. 1), from Visso to Campotosto (e.g. Tinti et al., 2016; Chiaraluce et al., 2017), activating an 80-km long system of SW-dipping normal fault segments, along which spectacular co-seismic ruptures were observed. The structures involved, are part of a longer alignment of seismogenic faults, responsible of the main seismic sequences, which have affected the region for the last 40 years (e.g. Boncio et al., 2004; Barchi and Mirabella, 2009). They are also responsible for significant historical seismicity (Rovida et al., 2020). Hundreds of thousands of earthquakes were registered during the 2016–2017 sequence (e.g. Chiaraluce et al., 2017; Improta et al., 2019), including 9 events with Mw > 5 (Fig. 1b). The sequence started on August 24, 2016 with the Mw 6.0 Amatrice earthquake, close to the town of Accumoli (Michele et al., 2016; Tinti et al., 2016), causing intense ground shaking and a cm-scale surface rupture along the M. Vettore normal fault trace (Pucci et al., 2017). Following two months of continuous aftershock activity, on October 26, the Mw 5.9 Visso earthquake occurred at the north-western edge of the aftershock area. Four days later (October 30), the strongest event of the sequence with Mw 6.5 occurred close to Norcia, halfway between the towns of Amatrice and Visso. Finally, on January 18, 2017, a series of four additional moderate magnitude (5.0 < Mw < 5.5) extensional earthquakes, hit the Campotosto area, in the southernmost part of the affected region (Fig. 1b).

This paper is aimed at providing a new, comprehensive reconstruction of the subsurface structure of the entire area affected by the 2016–2017 seismic sequence, as constrained by previously unreleased deep seismic data seismic profiles, giving insights into the influence of the subsurface geology (i.e. lithology and structure) on the geometry and seismicity patterns associated with the faults. The reconstruction is based on a set of five geological cross-sections, extrapolated down to a depth of about 12 km, oriented ca. N65°, orthogonal to the strike of the causative faults of the earthquakes. The sections are based on the integration of surface geological data, mostly derived from published maps (mainly Koopman, 1983; Centamore et al., 1992; Pierantoni et al., 2013) and seismic reflection profiles, acquired for oil exploration purposes in the late twentieth century (some of which are shown by Porreca et al., 2018). Earthquake foci are derived from a re-localized data-set (from Michele et al., 2020) and focal mechanisms come from INGV TDMT (web-service: http://cnt.rm.ingv.it/tdmt; Scognamiglio et al., 2009). Seismicity has been plotted along the cross sections so that the relationship between the geological and seismological faults (sensu Chiaraluce et al., 2005) can be assessed and discussed.

2. Regional framework and surface geological structures

The area associated with the 2016–2017 seismic sequence is located in a tectonically complex region, where three major structural domains interact (Fig. 1a), whose stratigraphy is schematically represented in Fig. 2:

- the *Umbria-Marche Domain*, i.e. the SE part of the Umbria-Marche fold-and-thrust belt (e.g. Barchi et al., 2001), involving a Mesozoic-Paleogene multilayer sequence of carbonate rocks (Umbria-Marche succession, e.g. Cresta et al., 1989; Centamore et al., 1992; Menichetti and Coccioni, 2013);
- the *Gran Sasso Domain*, representing the transition between the Umbria-Marche pelagic basinal area and the southernmost Latium-Abruzzi Platform, which is the source of the abundant calcareous turbidites, intercalated in the Mesozoic-Paleogene multilayer sequence (Ghisetti and Vezzani, 1991; Cardello and Doglioni, 2015);
- the *Laga Foredeep Domain*, where Late Miocene syn-orogenic siliciclastic deposits extensively crop out (Flysch della Laga Fm.; Centamore et al., 1992), covering the Umbria-Marche succession.

The structural evolution of this region is characterised by a Late Miocene-Early Pliocene compressional phase, followed by Late Pliocene–Quaternary extension (e.g., Ghisetti et al., 1993; Pauselli et al., 2006; Barchi, 2010; Cosentino et al., 2010; Beaudoin et al., 2020). The compressional structures show a very complex pattern (Fig. 1a). Both Umbria-Marche and Gran Sasso domains overthrust the Laga Foredeep Domain via major arcuate reverse faults: the Monti Sibillini (hereinafter MSt, Koopman, 1983; Lavecchia, 1985; Cooper and Burbi, 1986; Mazzoli et al., 2005) and Gran Sasso thrusts (e.g. Ghisetti and Vezzani, 1991), with eastward and northward convexity, respectively (Fig. 1a). The fold axes associated to these thrust systems mainly trend N-S in the Umbria-Marche and Laga Foredeep Domains, and WNW-ESE in the Gran Sasso Domain. At regional scales, the subsequent (mainly Quaternary) normal faults crosscut this complex assemblage of compressional structures, maintaining a regular, NNW-SSE alignment, across the whole study area. A set of intermountain basins (Fig. 1a; Barchi et al., 2000; Boncio et al., 2004), is generated in the subsiding hangingwalls of the faults (Calamita et al., 1992; Blumetti et al., 1993; Vignaroli et al., 2019), infilled by continental sediments of Quaternary and possibly late Pliocene (e.g. Cosentino et al., 2017) age.

Five geological cross-sections have been constructed across the study area (Fig. 3), oriented orthogonally to the strike of the major active normal fault systems (i.e. N65°), as expressed by the focal mechanisms of the mainshocks (Mw > 5) during the sequence and by the attitude of the major Quaternary normal faults exposed at the surface (Fig. 1).

Section S01 (Fig. 3a) crosses the NW termination of the Cupi-Ussita Fault (Brozzetti et al., 2019), the northernmost segment activated during the sequence. The section also crosses the southernmost fault segments (Mt. Cavallo-Mt. Fema fault segments, Chiaraluce et al., 2005) activated during the 1997–1998 Umbria-Marche sequence (Sellano earthquake, Mw = 5.5, 14th October 1997, e.g. Chiaraluce et al., 2003). Sections S02, S03, S04 and S05 pass through the hypocentres of four major events of the Amatrice-Visso-Norcia 2016–2017 sequence. Section S02 (Fig. 3b) crosses the Mt. Bove Fault, close to the 26th October 2016 (Mw = 5.9) hypocentre. Section S03 (Fig. 3c) crosses the M. Vettore Fault, close to the 30th October 2016 $M_W = 6.5$ hypocentre. Section S04 (Fig. 3d) crosses the 24th August 2016 (Mw = 6.0) hypocentre that occurred in the area corresponding to the transfer zone between the SE termination of the M. Vettore Fault and the NW termination of the M. Gorzano Fault (see map in Fig. 1a). Section S05 (Fig. 3e) crosses the Campotosto Fault, i.e. the last and southernmost segment of the system, activated on the 18th of January 2017 by 4 events with 5.0 < Mw < 5.5. About 10 km west of the Campotosto Fault, the S05 section also crosses the Montereale Fault, another Quaternary structure which is believed to be active and seismogenic (Civico et al., 2016; Cinti et al., 2018).

The major compressional and extensional structures of the study area are described in the following sections, based on the authors' extensive geological knowledge of the region derived from fieldwork, as well as on previously published geological maps (e.g. Centamore et al., 1992; Pierantoni et al., 2013; Testa et al., 2019; Stendardi et al., 2020).

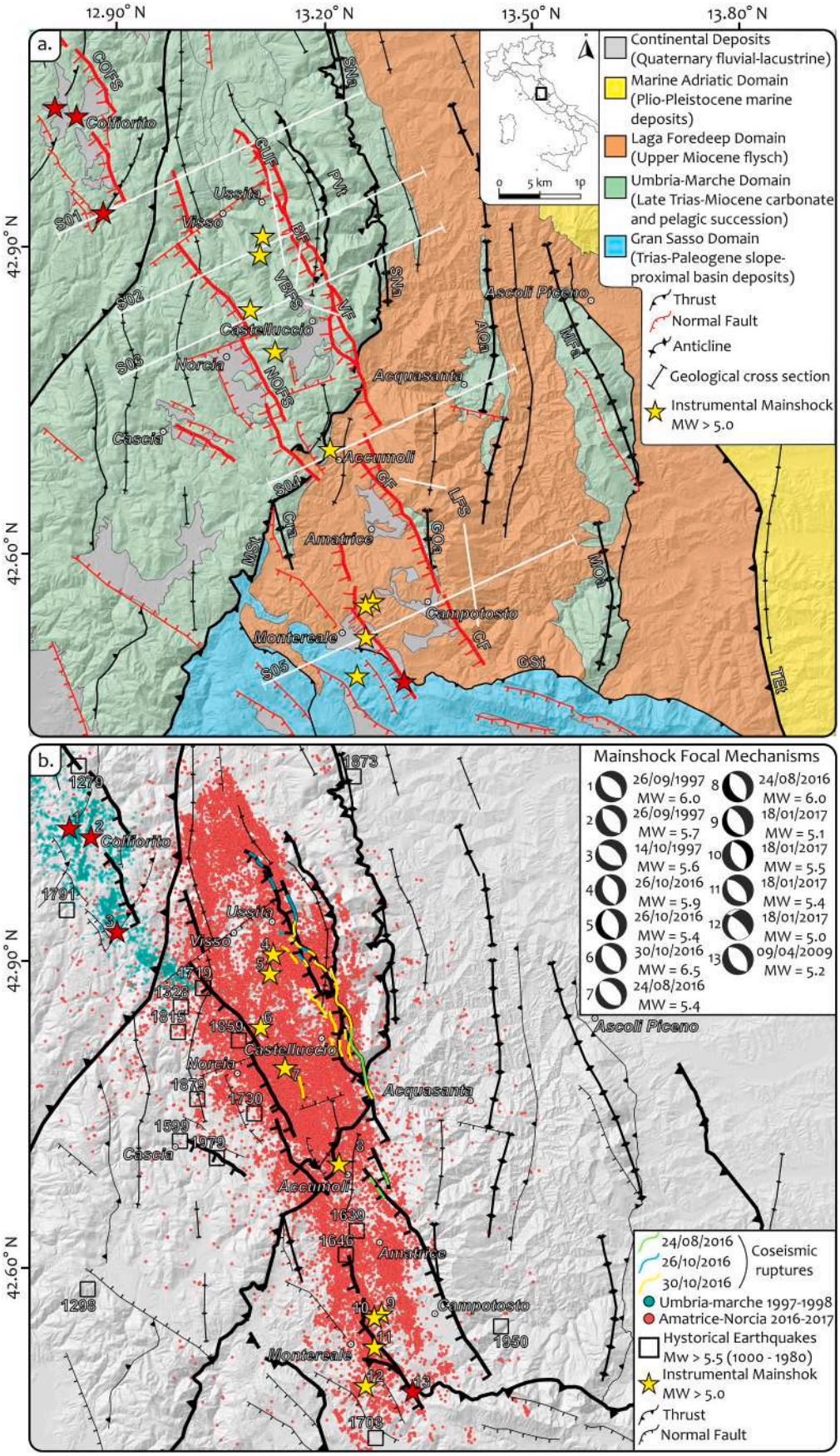

Fig. 1. Geology and seismicity of the study area. (**a**) Structural sketch, showing the main compressional and extensional features of the study area, the traces of the geological cross sections of Figure 3 (S01 to S05) and the mainshock epicentres (Mw > 5.0) of the Accumoli-Amatrice 2016–17 sequence (in yellow) and of the previous Colfiorito 1997–98 and L'Aquila 2009 sequences (in red). Major Thrusts: Monti Sibillini thrust (MSt) – Gran Sasso thrust (GSt); Pizzo Tre Vescovi thrust (PVt), Teramo thrust (TEt). Major anticlines of the Laga Domain: Sarnano ant. (SNa); Cittareale ant. (CRa); Acquasanta ant. (AQa); M. Gorzano ant. (GOa); Montagna dei Fiori ant. (MFa); Montagnone ant. (MOa). Major Normal Faults: Colfiorito Fault System (COFS); Norcia Fault System (NOFS); Vettore-Bove Fault System (VBFS), with its segments Cupi-Ussita Fault (CUF), M. Bove Fault (BF) and M. Vettore Fault (VF); Laga Fault System (LFS), with its segments M. Gorzano Fault (GF) and Campotosto Fault (CF). (**b**) Seismicity map, showing the instrumental seismicity of the Accumoli-Amatrice 2016–17 (in red) and of the Umbria-Marche 1997–98 (in cyan) sequences, and the historical seismicity in comparison with the major compressional and extensional structures of the study area; the co-seismic ruptures are also reported, after Brozzetti et al. (2019), Ferrario and Livio (2018) and Galli et al. (2019) (For interpretation of the references to color in this figure legend, the reader is referred to the web version of this article.)

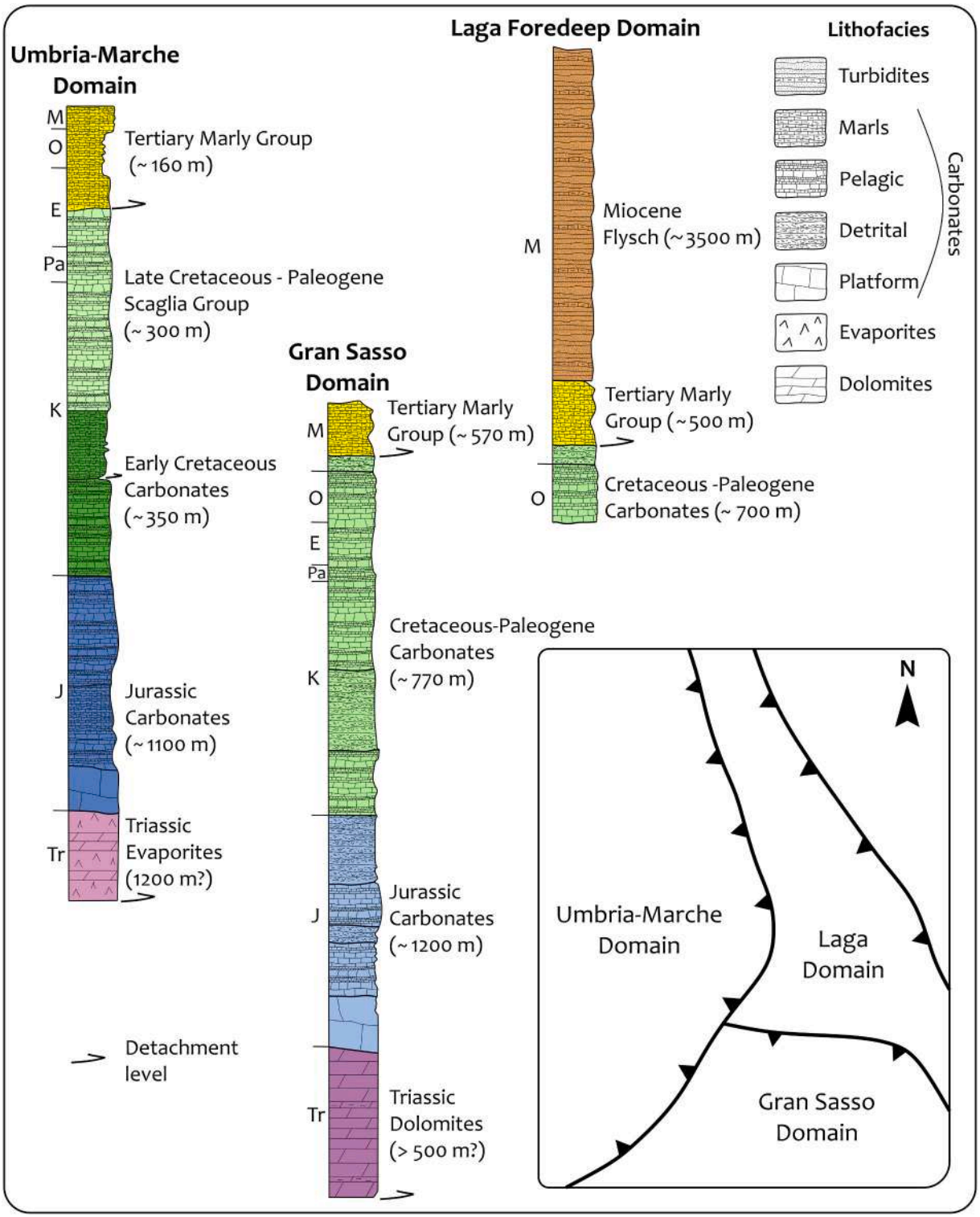

Fig. 2. Schematic stratigraphic columns, representative of the three major domain of the study area. The columns (not to scale) do not keep into account significant lateral variations affecting the sedimentary successions. The columns derive from Menichetti and Coccioni (2013) for the Umbria-Marche Domain, and from Cardello and Doglioni (2015) for the Gran Sasso and Laga domains. The inset map shows the distribution and structural relationships between the three domains.

2.1. *Compressional structures*

In the Umbria-Marche Domain, the Umbria-Marche succession extensively crops out in the hangingwall of the MSt, forming a complex pattern of box shaped *E*-verging folds and arcuate thrusts (Fig. 1a). The overall shortening direction is ca. E-W (N80°E), as evidenced by the N-S trending fold axes and by the kinematic indicators on the major thrust faults (e.g. Lavecchia, 1985; Barchi, 1991). The sections S01, S02 and S03 (Fig. 3a,b,c) illustrate the structural style of these compressional structures, which correspond to the 'Umbria-Marche folds' (Massoli et al., 2006), detached within the Triassic evaporites (Burano Fm.; Martinis and Pieri, 1964) and involving the whole carbonatic succession, with a typical wavelength of 4–6 km (Massoli et al., 2006).

In the Laga Foredeep Domain, the Messinian Laga turbidites

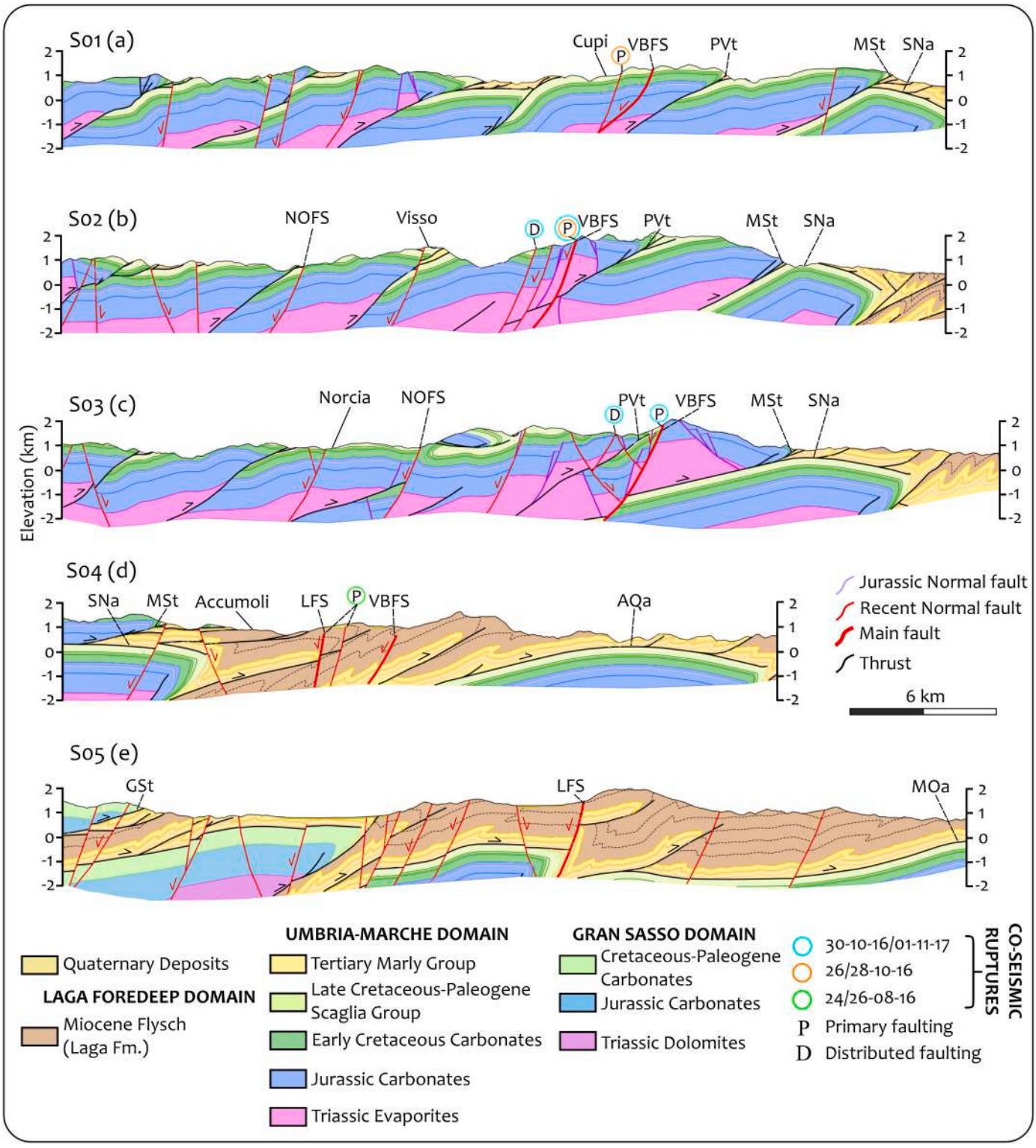

Fig. 3. Geological cross-sections across the study area. The reconstruction of the shallow geological structures is based on available geological maps and literature data (Koopman, 1983; Centamore et al., 1992; Pierantoni et al., 2013; Carta Geologica Regionale 1:10000 – Regione Marche, 2014; Carta Geologica Regionale 1:10000 – Regione Umbria, 2016). The legend of the major compressional and extensional structures is the same of Fig. 1a.

extensively crop out, with a maximum thickness exceeding 3 km in the major synclines. The underlying Umbria-Marche succession is involved in a series of 3 major N-S trending anticlines, generated in the hanging-wall of W-dipping major thrusts, from W to E: Sarnano-Cittareale, Acquasanta-Gorzano and Montagna dei Fiori-Montagnone Anticlines (Fig. 1a). As also observed by Massoli et al. (2006) in other areas where the Umbria-Marche succession is covered by thick turbidites successions, these folds involving the carbonates are here spaced at a much larger wavelength (10–15 km) than in the Umbria-Marche Domain (Sections S04 and S05, Fig. 3d,e). The Laga turbidites are generally detached from the underlying Umbria-Marche succession by the Laga Detachment Zone (sensu Koopman, 1983), generating low-wavelength

folds and imbricates, also imaged in the sections S03, S04 and S05 (Fig. 3c,d,e).

In the southern part of the study area, the WNW-ESE trending Gran Sasso thrust (e.g. Ghisetti and Vezzani, 1991; Cardello and Doglioni, 2015) marks the boundary between the Laga Foredeep and Gran Sasso domains (Fig. 1a). South of the structurally complex zone, where the western termination of the Gran Sasso thrust meets the MSt, the latter assumes the characteristics of a major transpressive fault (Olevano-Antrodoco tectonic Line, e.g. Salvini and Vittori, 1982).

2.2. Extensional structures

In the Central Apennines, Quaternary extension is accommodated by a composite pattern of NNW-SSE trending, mostly WSW-dipping, seismogenic normal faults (Fig. 1; e.g. Barchi et al., 2000; Boncio et al., 2004). Since the Late Pliocene–Early Pleistocene, displacement along these extensional faults have led to the formation of a series of narrow continental basins (Calamita et al., 1994; Cavinato and De Celles, 1999; Lavecchia et al., 1994, 2002; Cosentino et al., 2017). The basins located in the study area are: the Cascia, Norcia and Castelluccio di Norcia basins (Calamita et al., 1982; Blumetti et al., 1993; Brozzetti and Lavecchia, 1994; Coltorti and Farabollini, 1995), in the Umbria-Marche Domain; and the Amatrice (Vignaroli et al., 2019) and Montereale (Chiarini et al., 2014) basins in the Laga Foredeep Domain (Fig. 1a).

The main seismogenic normal faults in the study area, are arranged into two main sub-parallel alignments, separated across strike by a distance of about 10 km (Fig. 1). The western, longer alignment (~ 200 km long) affects the whole Umbria region from Città di Castello to Norcia, extending southward to Montereale and L'Aquila (e.g. Barchi et al., 2000; Boncio et al., 2004). This system includes the main normal faults responsible for the Mw 5.8 Norcia 1979 (Deschamps et al., 1984), the Mw 5.4 Gubbio 1984 (Valensise and Pantosti, 2001), the Mw 6.0 Colfiorito 1997 (Chiaraluce et al., 2003), and the Mw 6.1 L'Aquila 2009 (Valoroso et al., 2013) earthquakes. In this study, we mostly focus on the eastern alignment, activated during the 2016–2017 seismic sequence, which consists of two major sets of active faults (Fig. 1a): the M. Vettore-M. Bove Fault System (VBFS), including the Cupi-Ussita (CUF), M. Bove (BF) and M. Vettore (VF) fault segments; and the Laga Fault System (LFS), including the M. Gorzano (GF) and the Campotosto (CF) fault segments. It is worth noting that different interpretations of the LFS segmentation have been proposed in previous studies (Boncio et al., 2004; Falcucci et al., 2018). At the surface, the boundary between the VBFS and LFS grossly corresponds to the MSt, even though detailed geological mapping showed that the M. Vettore Fault displaces the MSt, propagating few km across the Laga Foredeep Domain (Porreca et al., 2020; Stendardi et al., 2020 and references therein). The geomorphological expression of the active normal faults is much more evident in areas where carbonate rocks crop out (e.g. Umbria-Marche Domain), compared to areas where the bedrock consists of turbidite sandstones and marls (e.g. Laga Foredeep Domain).

The seismogenic activity of these faults is demonstrated, beyond the evident spatial connection with the instrumental seismicity distribution (e.g. Chiaraluce et al., 2005), by the historical seismicity (summarised in the national catalogues by Rovida et al., 2016, 2020) and by several paleo-seismological studies (e.g. Galli et al., 2008, 2017; Cinti et al., 2011). Such data also demonstrate the seismogenic activity of other nearby fault segments, like Cascia and M. Alvagnano faults (Blumetti and Guerrieri, 2007; Galli et al., 2020) and Montereale fault (Chiarini et al., 2014; Civico et al., 2016; Cinti et al., 2018).

The position and associated net displacement of the major normal faults affecting the study area are also represented along the five geological sections of Fig. 3, and the position of the surface ruptures, mapped after the 2016–2017 seismic sequence are also shown (Ferrario and Livio, 2018; Villani et al., 2018, 2018a; Brozzetti et al., 2019; Galli et al., 2019).

3. Seismic reflection data

The geological reconstructions proposed in this paper are based on a wide date-set of about 100 2-D seismic data seismic reflection profiles, acquired in the study area in the last decades of the 20th century (1970–1998) for oil exploration purposes (Fig. 4a). Most of these lines, never published before, were kindly provided by the Italian oil company (ENI S.p.A.), whilst others were extracted from the public database "Visibility of petroleum exploration data in Italy" (Videpi Project, www.videpi.com). From the same sources, we extracted the stratigraphy of 4 deep boreholes (Varoni1, Campotosto1, Antrodoco1 and Amandola1, see locations in Fig. 3a), drilled in the study area. A more complete description of the data-set, including details of the acquisition and processing techniques, was provided in Porreca et al. (2018). Despite the quite irregular spatial distribution of the seismic profiles and their variable resolution, these data provide unique images of some representative structures, giving relevant insights into the geological setting at depth and the structural style of both compressional and extensional features.

3.1. Seismic stratigraphy

The definition of a coherent, easily applicable seismic stratigraphy is an essential, preliminary step for any seismic interpretation procedure. Following on from previous seismic reflection studies performed in Central Italy (e.g., Bally et al., 1986; Barchi et al., 1998; Bigi et al., 2011; Mirabella et al., 2008, 2011), four main seismo-stratigraphic units are defined here in the study area (Fig. 4b), characterised by distinctive seismic facies and calibrated using the few available deep boreholes. The units are described as follow, from top to bottom.

The uppermost unit ('*Turbidites*') includes the Miocene Flysch (MF) of the Messinian Laga Fm. (e.g. Centamore et al., 1992) and the underlying Early Tertiary Marly Group, (Koopman, 1983; Cooper and Burbi, 1986). In the nearly undeformed sections (e.g. in syncline hinge zones), the Laga Fm. sandstones are characterised by a regular set of high-frequency reflectors, with good lateral continuity, overlaying the nearly transparent facies of the Tertiary Marly Group (Fig. 4c). In most profiles, however, the seismic facies of the Turbidites is more chaotic, reflecting their intense folding and fracturing.

The second unit ('*Carbonates*') corresponds to the Mesozoic-Paleogene Umbria-Marche succession (UC, Fig. 4b), including the Cretaceous–Paleogene Carbonates (Scaglia Group and the underlying Early Cretaceous Carbonates, Fig. 2) and the Jurassic Carbonates. It is characterised by an overall transparent seismic facies, with two major high amplitude and continuous reflections in the upper part, corresponding to the top of the Scaglia Group (Top UC, Fig. 4b) and to the mid-Cretaceous marly horizon of Marne a Fucoidi Fm. (Top FUC, Fig. 4b); other reflectors are locally present in the central part of the unit (Fig. 4b, d).

The third unit ('*Evaporites*'), mainly corresponding to the Late Triassic Anidriti di Burano Fm. (Martinis and Pieri, 1964), is generally characterised by transparent seismic facies, often topped by a major reflector (Top TE, Fig. 4b), possibly corresponding to a relatively thin horizon of layered dolomitised limestones and marls (Calcari e Marne a Rhaetavicula Contorta Fm., Ciarapica, 2007).

The deepest unit, the underlying *'Basement*' never crops out in this region and is drilled by few deep boreholes, scattered across the Italian peninsula (see e.g. Patacca et al., 2008). The uppermost part of the Basement consists of sedimentary or low-grade metamorphosed clastic successions of Late Palaeozoic-Middle Triassic age (phyllites), and is characterised by a set of oblique, medium to high amplitude, low-continuity reflections, contrasting with the overlying transparent facies of the Evaporites. These peculiar seismic facies have been referred to previously as the 'acoustic basement' (Bally et al., 1986; Barchi et al., 1998; Mirabella et al., 2008).

The V_P interval velocities reported in Fig. 4b, used for the depth

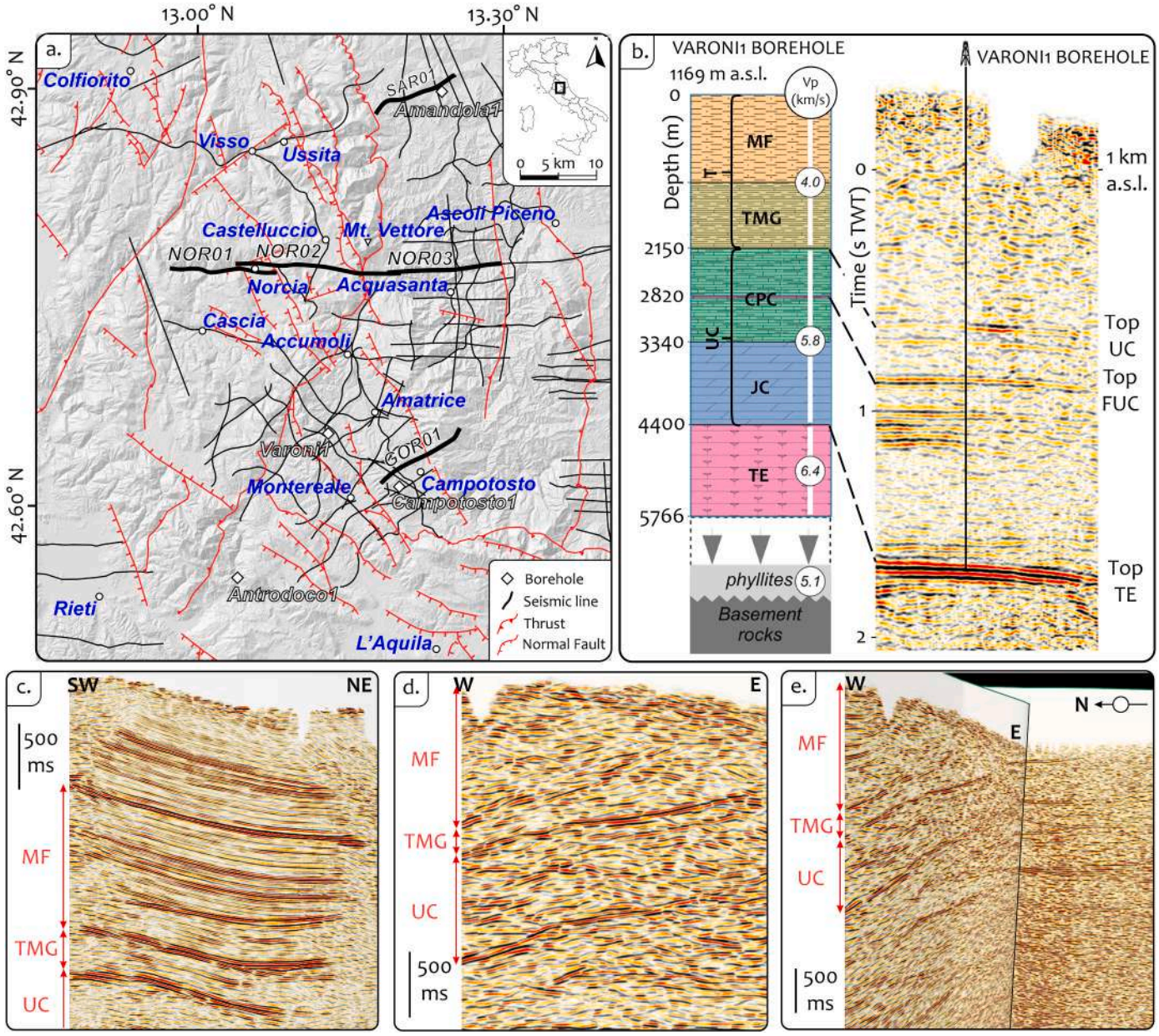

Fig. 4. Seismic reflection data and seismic stratigraphy. (**a**): Location map of the seismic reflection profiles and wells used in this study; thick lines are the traces of the seismic profiles shown in Figure 5, 6 and 7; (**b**): calibration of the seismic reflection profile with the Varoni 1 well stratigraphy showing: i) the Turbidites unit, divided in Miocene Flysch (MF, Laga Fm.) and Tertiary Marly Group (TMG), ii) the Umbria Carbonates (UC) divided in the Cretaceous-Paleogene Carbonates (CPC) and Jurassic Carbonates (JC), iii) the Triassic Evaporites (TE); (**c**), (**d**) and (**e**): representative examples of seismic stratigraphy, extracted from the lines SAR01 (c), NOR03 (d), and at the intersection between NOR03 and an orthogonal profile (e).

conversion of the seismic profiles interpreted in this study, are derived from well data, collected by the numerous previous studies performed in this region (Bally et al., 1986; Barchi et al., 1998; Bigi et al., 2011; Latorre et al., 2016). This regional data-base of the available velocity data was recently summarised and improved by Montone and Mariucci (2020).

3.2. Description of the seismic profiles

The examples illustrated in the present paper consists of five seismic reflection profiles, here named SAR01, NOR01, NOR02, NOR03 and GOR01 (see traces in Fig. 4a).

The original seismic reflection profiles (Porreca et al., 2018) have been improved in their quality and interpretability using a workflow combining data-preconditioning and attribute analysis (Chopra and Marfurt, 2007; Marfurt, 2018). This technique is a relatively cheap and fast strategy to qualitatively emphasize data properties and geophysical features in conventional seismic reflection datasets. An extensive overview and discussion on these techniques can be found in Ercoli et al. (2020).

In the present work, we have experimented using structure-oriented filters (i.e. dip-steering median filter) as a pre-conditioning strategy before computing the pseudo-relief attribute (Ercoli et al., 2020 and references therein). This process enhances laterally continuous events reducing the random noise, but without suppressing details of reflection events consistent with the structures. Our workflow had a fruitful effect on our seismic data, cleaning up the random noise characterizing the original seismic lines, better focusing the key reflected horizons. A good example of the substantial benefits gained by the application of this technique is observable in the line SAR01 in Fig. 5a, where despite the

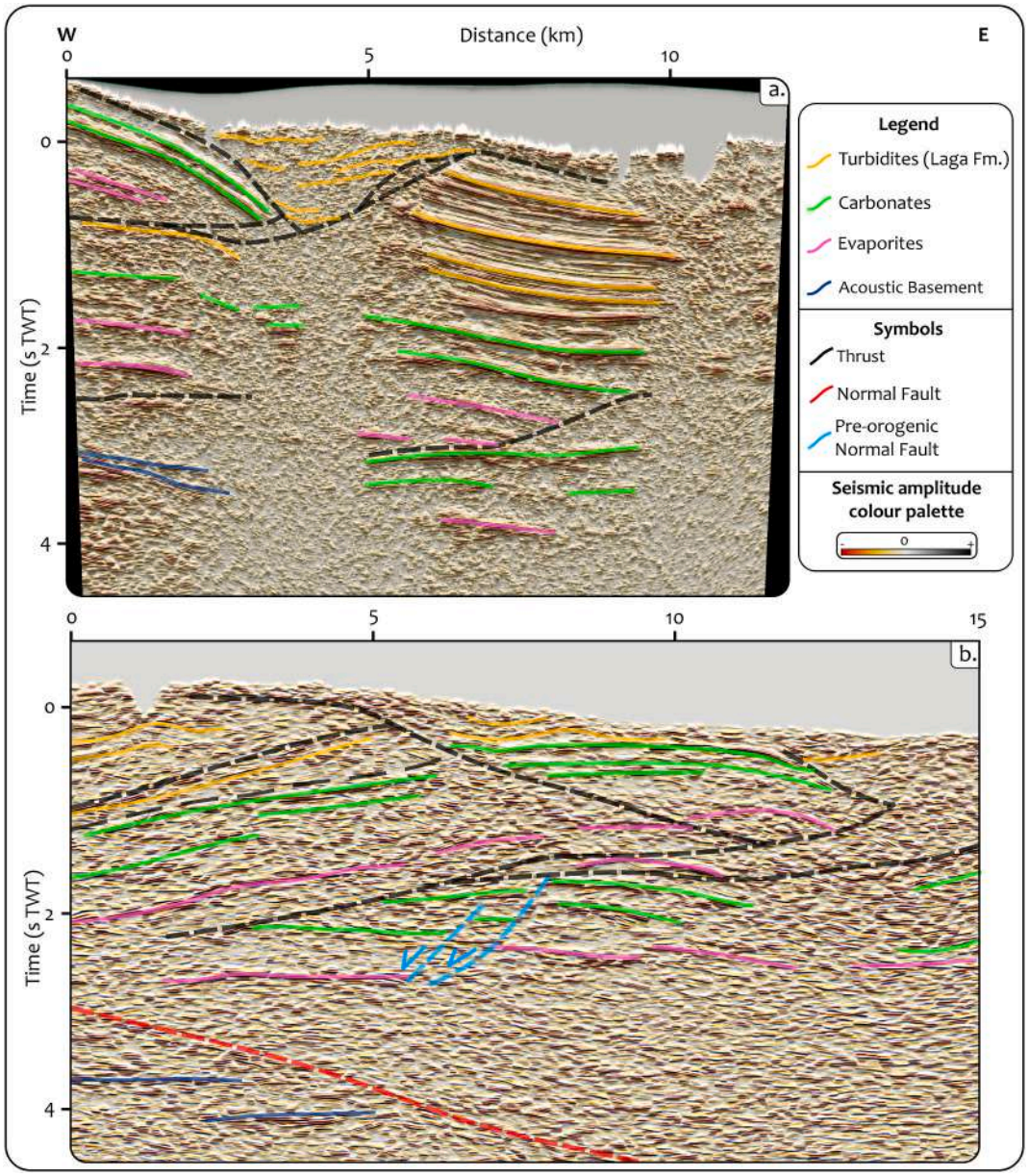

Fig. 5. Interpretation of the seismic profiles SAR01 and NOR03 (see trace on Figure 4). (**a**) Line drawing of the seismic profile SAR01. (**b**) Line drawing of the seismic profile NOR03. See text for the descriptions. The uninterpreted images are in the supplementary material (S1 and S2 respectively).

original low quality, contains sets of reflections have been positively enhanced allowing the key geological structures to be mapped. Thanks to this approach and following improvements, we propose some novel interpretations, including seismic profiles (e.g. NOR01, NOR02 and NOR03) already described and discussed by Porreca et al. (2018) and Ercoli et al. (2020).

The seismic profile SAR01 (Fig. 5a) crosses the Sarnano area, in the footwall of the MSt, and extends ENE-ward (ca. N75°) across the Laga basin (Figs. 1 and 4a). In the shallower part of the profile, the east-dipping forelimb of a major anticline involving the Carbonates, is clearly imaged (Sarnano anticline, Cooper and Burbi, 1986, see map in Fig. 1), overthrusting a thick (about 2 s TWT), nearly undeformed siliciclastic succession. In the thrust hangingwall, the internal reflection of the Turbidites are strongly deformed and totally detached from their original substrate, forming a triangle zone between a W-dipping out-of syncline thrust and an E-dipping forelimb back-thrust. In the deeper portion of the profile, a second unit of Carbonates can be recognized beneath the Sarnano anticline, connected towards the east to the exposed bedrock of the Laga succession. Beneath the Carbonates and the Evaporites, between 3 and 4 s TWT, reflective seismic facies are interpreted to represent the acoustic basement. In the central part of the profile, a major, gently W-dipping reflection obliquely dissects the stratigraphic markers of the Carbonates at a depth of about 3 s twt: this reflection was interpreted as a major thrust, producing the observed tectonic duplication of the Carbonates.

The E-W trending seismic profile NOR03 (Fig. 5b) crosses the Acquasanta anticline just 2 km north of Acquasanta village (Figs. 1 and 4a), providing another well resolved image of the subsurface structures of the Laga Foredeep Domain. The Acquasanta anticline, involving the Carbonates and the underlying Evaporites, is here imaged as a large asymmetric, east-verging box-fold. It shows a long, gently W-dipping back-limb and a relatively flat crestal zone, separated by a steep, E-dipping back-thrust. The short forelimb is poorly imaged, presumably because its strata are very steep or even overturned. A set of short-wavelength folds and imbricated thrusts, with a marked eastward tectonic vergence, involve the Turbidites on top of gently W-dipping

Carbonates of the Acquasanta anticline back-limb. The overall geometry of the anticline, as imaged by the Carbonate reflectors, is quite similar to that of the widely described major anticlines exposed in the Umbria-Marche Domain (e.g. Calamita and Deiana, 1988; Lavecchia et al., 1988; Calamita et al., 1994; Tavarnelli, 1997; Mazzoli et al., 2005; Calamita et al., 2012). The anticline is generated at the hangingwall of a major W-dipping fore-thrust, with a staircase trajectory, suggesting a fault-bend-fold mechanism (e.g. Calamita et al., 2012), with a basal decollement located within the Evaporites. At the footwall of the thrust, beneath the crest zone of the box fold, the seismic profile shows a set of gently E-dipping reflections, down to at least 2.5 s (TWT), affecting a deeper Carbonate Unit. Within this unit, the reflectors are displaced by a set of W-dipping normal faults, apparently pre-dating the emplacement of the thrust.

The NOR01 and NOR02 seismic profiles (Fig. 6) extend in an E-W direction along the westward continuation of the profile NOR03, crossing the Quaternary basins of Norcia (Nb) and Castelluccio di Norcia (CNb) and the faults bordering them, as shown in the pseudo-3D view of Fig. 6a.

The profiles (Fig. 6b, c) offer a view of the conjugate high-angle normal fault systems bordering the Quaternary basins, imaged as steep alignments of disrupted reflectors, that clearly corresponds to the position of the faults mapped at the surface (see e.g. Brozzetti and Lavecchia, 1994 for Nb and Pierantoni et al., 2013 for CNb). The eastern part of profile NOR01 (Fig. 6b) images the master faults bordering the flanks of the asymmetric Nb, i.e.: the SW-dipping Norcia Fault, bordering its eastern flank and its major, antithetic (i.e. NE-dipping) splay, bordering the western flank. The Norcia Fault is also visible in the NOR02 profile (Fig. 6c), whose central portion images the main faults, bordering the CNb. The master fault is here represented by the SW-dipping M. Vettore Fault, reactivated during the 2016 earthquake (e.g. Villani et al., 2019), whilst the main NE-dipping, antithetic normal fault, joins onto the M. Vettore Fault at about 2–3 s. A further, major antithetic blind fault can be traced west of CNb, which was proposed to be responsible for a large aftershock (Mw 5.4) that occurred few hours after the 24th August Amatrice main shock (Chiaraluce et al., 2017; Porreca et al., 2018; Improta et al., 2019).

For both Nb and CNb, the seismic volume between the two, opposite

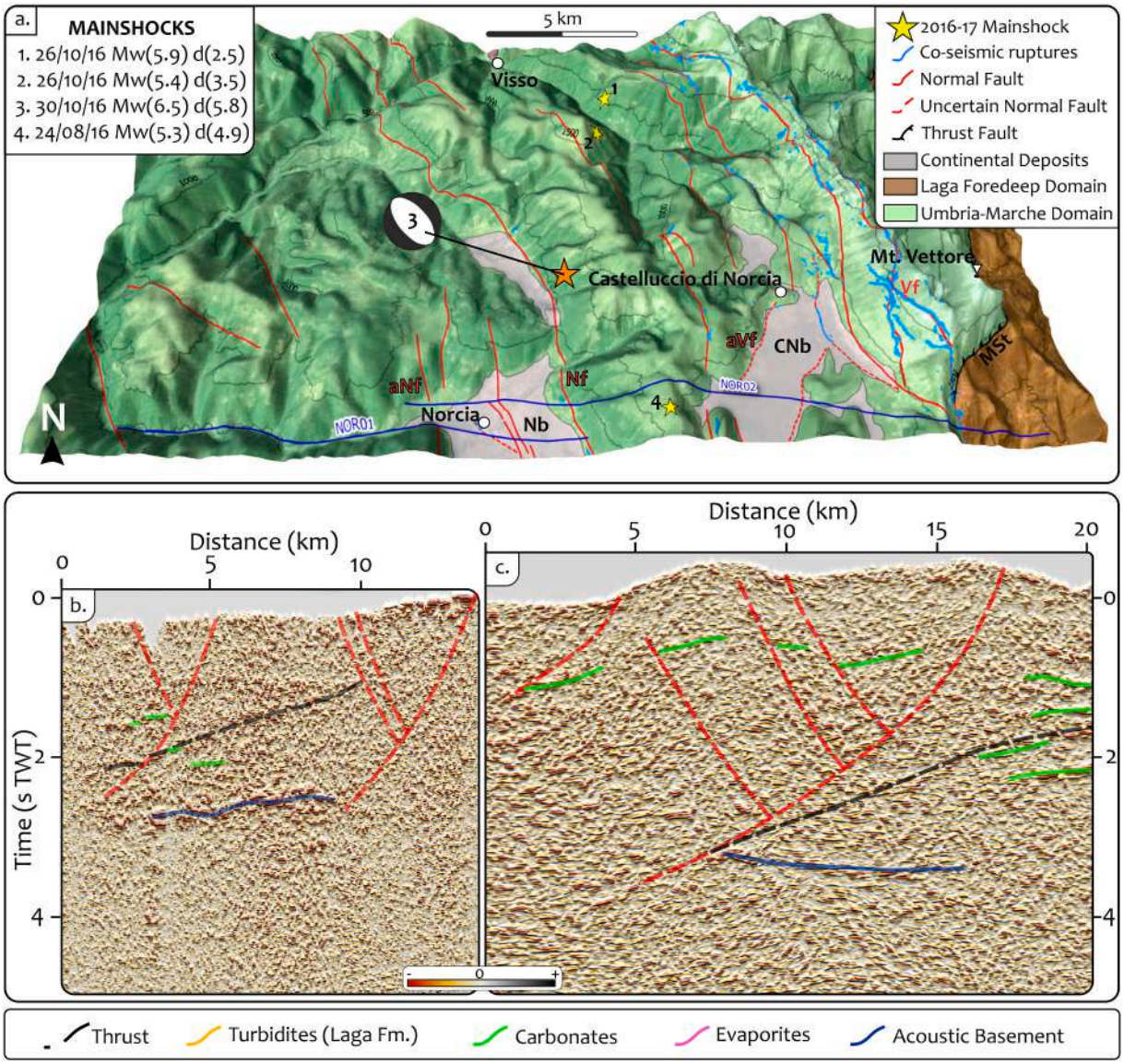

Fig. 6. Interpretation of the seismic profiles NOR01 and NOR02 (see trace on Figure 4). (**a**) 3D geological sketch of the Norcia-M.Vettore area, showing the mainshocks, the main tectonic structures and the co-seismic ruptures. aNf is the antithetic fault of the Norcia Fault (Nf); aVf is the antithetic fault to the Vettore Fault (Vf); Norcia basin (Nb); Castelluccio di Norcia basin (CNb); Mt. Sibillini thrust (MSt). (**b**) Line drawing of NOR01. (**c**) Line drawing of NOR02. See text for the description. The uninterpreted images are in the supplementary material (S3 and S4 respectively). Modified after Ercoli et al. (2020).

dipping, conjugated normal faults, shows a peculiar reflection fabric, dominated by high-angle discontinuities (Fig. 6b, c). This is interpreted to represent penetrative systems of minor, synthetic and antithetic splays (Ercoli et al., 2020), in good correspondence with the complex pattern of Quaternary faults mapped at the surface (e.g. Pierantoni et al., 2013), as well as with the dense network of co-seismic ruptures that occurred in this area (distributed deformation, sensu Ferrario and Livio, 2018). Several minor fault splays, affecting the bedrock and deposits of the CNb, were also revealed by near-surface geophysical surveys, performed before and after the occurrence of the seismic sequence (e.g. Ercoli et al., 2013, 2014; Villani et al., 2019).

In the deeper parts of both sections, at around 3 s twt, a prominent reflection has been recognized (Fig. 6b, c), particularly evident along the NOR02 profile, beneath CNb, where it has been previously interpreted (Porreca et al., 2018; Ercoli et al., 2020) as corresponding to the top of the acoustic basement. The continuity of the top basement is abruptly interrupted in its western edge, where two different tectonic structures converge: a low-angle west-dipping discontinuity, corresponding to the Sarnano thrust, which upward cuts the Carbonates reflectors of the backlimb of the Acquasanta Anticline; and a steeper discontinuity, following the trajectory of the M. Vettore Fault at depth. The crosscutting relationships between these two discontinuities are ambiguous and discussed in detailed by Ercoli et al. (2020).

The GOR01 seismic profile (Fig. 7) is not part of our data-set, but is derived from the paper by Bigi et al. (2013). Here we propose a new interpretation of this profile, that differs from that offered by Bigi et al. (2011, 2013). Bigi et al. (2013), Fig. 3b) propose that the active Campotosto fault (i.e. the southern segment of the Laga Fault System, Fig. 1a), exposed at the surface, is detached at a relatively shallow depth (about 4 km) and is not connected to the source of the earthquakes at depth. Consequently, the authors interpret its present-day activity as a "sympathetic reactivation induced by the motion of the deeper, seismogenic normal fault". This interpretation is compatible with the seismic signals, and explains the lack of shallow aftershocks. In our alternative interpretation (Fig. 7), the Campotosto Fault propagates downward to seismogenic depth, following the perfect alignment between the normal fault trace, exposed at the surface, and the deep seismicity, registered during both 2009 (e.g. Valoroso et al., 2013) and 2016–17 (e.g. Michele et al., 2020) sequences. In this interpretation, the geometry of the Campotosto Fault is similar to that of the other seismogenic normal faults, activated during the 2016–2017 sequence.

Moreover, we propose a new interpretation of the relationships between the M. Gorzano anticline and the Campotosto Fault, hypothesising that the anticline exposed at the surface in the footwall of the Campotosto Fault is a shallow structure, affecting only the detached Turbidites. This interpretation is based on the geology mapped at the surface (Centamore et al., 1992), showing that the N-S trending M. Gorzano anticline, involving the Carbonates, is actually displaced by the NNW-SSE trending Campotosto Fault (Fig. 1): south of the intersection point, the crest of this deeply-rooted anticline is downthrown in the hangingwall of the Campotosto Fault.

3.3. Summary

The available seismic profiles provide significant insights onto the structural style of both compressional and extensional structures.

The compressional structures are dominated by a consistent style of deformation, characterised by multiple décollements (Massoli et al., 2006). Two main décollements are clearly imaged in the seismic profiles:

- a shallower décollement is located in the Tertiary Marly Group, above the top of the Carbonates (Laga Detachment Zone, sensu Koopman, 1983) and generates intense, short-wavelength, disharmonic folding and imbrication of the Turbidites (lines SAR01, NOR03, GOR01);
- a deeper décollement is located within the Evaporites, generating long-wavelength, box-shaped anticlines involving the Carbonates (e.g. Sarnano and Acquasanta Anticlines). These anticlines developed in the hangingwalls of shallow-dipping major thrusts, are characterised

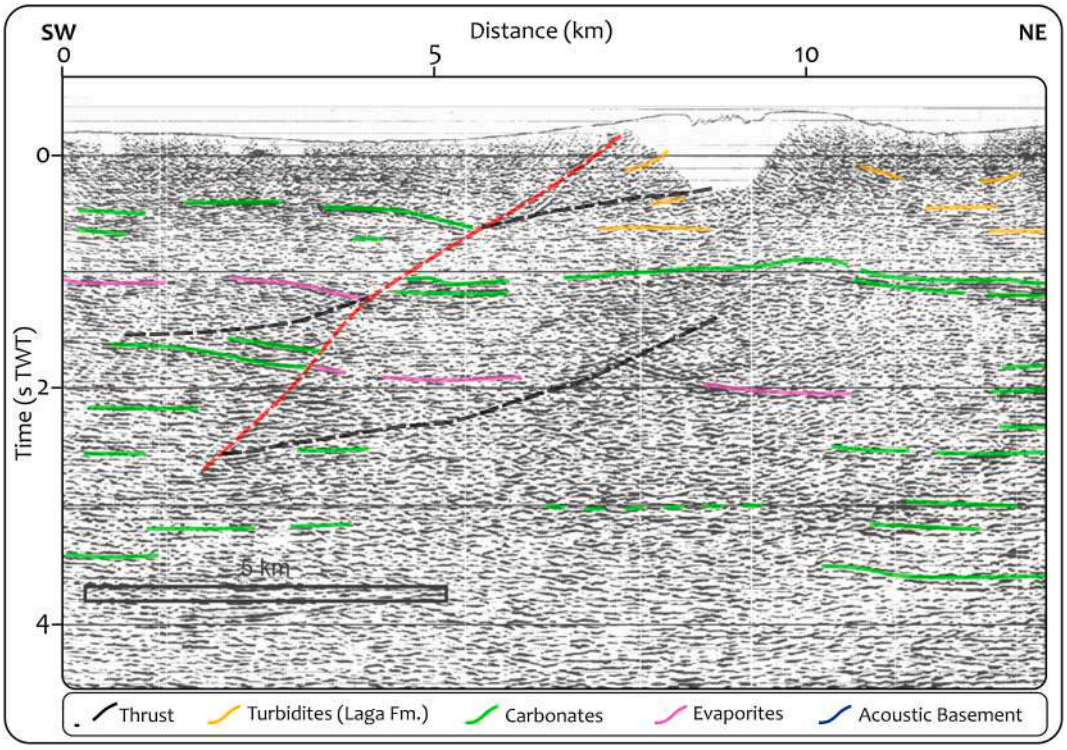

Fig. 7. Interpretation of the seismic profile GOR01 (see trace on Figure 4). See text for the description. The uninterpreted image is in the supplementary material (S5).

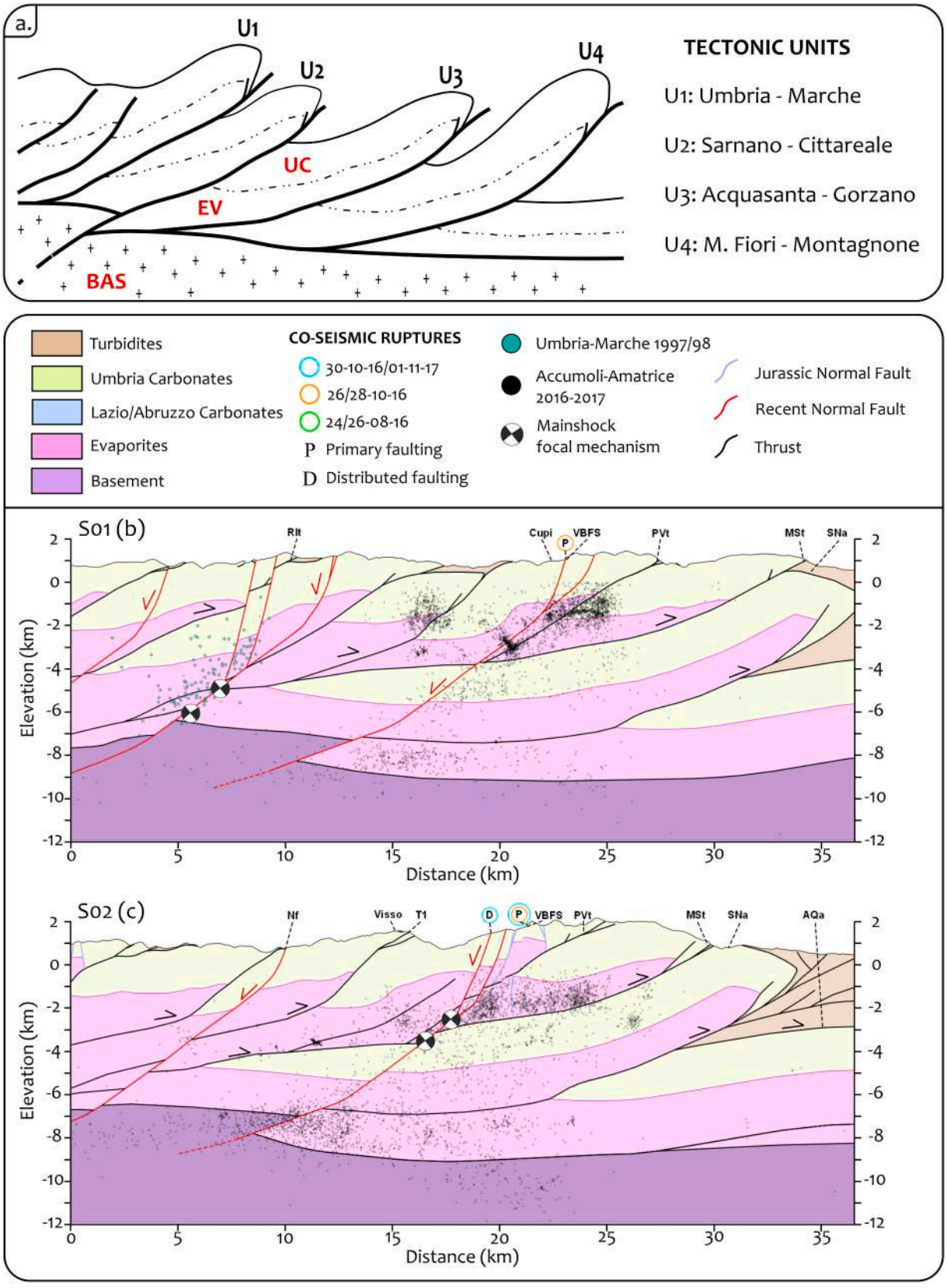

Fig. 8. Pg.2. Geological sections across the study area, extrapolated to seismogenic depth (see traces in Fig. 1a). Instrumental seismicity registered during the 2016–2017 sequence has been plotted into the sections. The legend of the major compressional and extensional structures is the same of Fig. 1a. The inset **(a)** is a conceptual scheme (not in scale) showing the relationships between the four main tectonic units of the study area: Umbria-Marche (U1), Sarnano-Cittareale (U2), Acquasanta-Gorzano (U3), and Montagna dei Fiori-Montagnone (U4). UC: Umbria-Marche carbonates, EV: Evaporites, BAS: Basement.

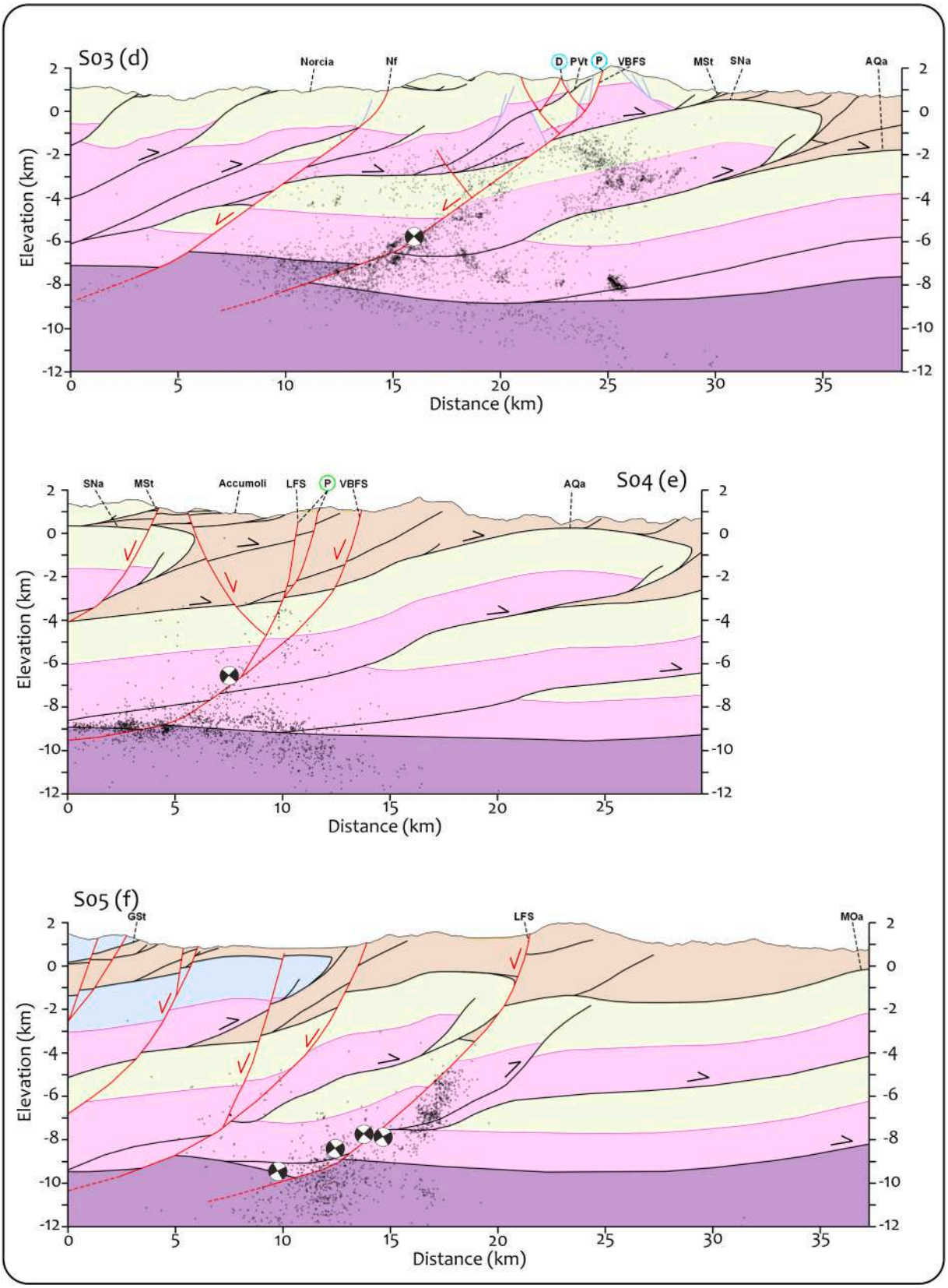

Fig. 8. (*continued*).

by significant amount of shortening (up to 10 km) and extensive duplication of the Carbonates (lines SAR01, NOR03).

The profiles also show that the top of the acoustic basement is not laterally continuous, suggesting that at least the uppermost part of the basement is deformed. Previous papers, based on seismic reflection

profiles, show that the top basement steps downwards to the east due to thrusting (Sage et al., 1991; Barchi et al., 1998; Fantoni and Franciosi, 2010).

The extensional structures (i.e. the active normal faults) cross-cut the stacked units of the sedimentary cover, from the surface down to the top Basement (lines NOR01, NOR02, GOR01), where they may reactivate the steps generated by the major thrusts. The extensional systems usually consist of conjugate sets, driven by SW-dipping master faults (NOR01, NOR02).

4. Integrated geological sections

The five geological sections, shown in Fig. 3, have been extrapolated down to ca. 12 km (Fig. 8), using the interpretation of the nearest available seismic reflection profiles and, more generally, the crucial indications offered by key-seismic profiles (see Chapter 3), in particular about the structural style at depth (e.g. thin vs. thick-skinned tectonics, Pfiffner, 2017; Poblet and Lisle, 2011) and the depth to basement.

Quite different reconstructions have been published previously by different authors for this area, proposing a large range of possible solutions for both the structural style and for the amount of the associated shortening (e.g. Ghisetti et al., 1993; Calamita and Pizzi, 1994; Bigi et al., 1999, 2011; Scisciani et al., 2014). A review of the previous studies about the structural setting of the region at depth was recently offered by Porreca et al. (2018). For our cross sections, we adopted a consistent structural style extensively observed throughout the region, characterised by a system of multiple décollements, where different sets of structures are generated at different structural levels, as described earlier.

Along our cross sections, the main compressional structures consist of four major stacked tectonic units, involving the Triassic-Paleogene Carbonates and Evaporites (Fig. 8a). Top to bottom (i.e. W to E), they are: the *Umbria-Marche Unit* (U1, at the hangingwall of the MSt), the *Sarnano-Cittareale Unit* (U2), the *Acquasanta-Gorzano Unit* (U3) and the *Montagna dei Fiori-Montagnone Unit* (U4). In the southernmost part of the study area, the Umbria-Marche Unit is replaced by the Gran Sasso Unit as the uppermost stacked unit U1. In the shallower and easternmost part of the sections, above the Carbonates, the Tertiary Turbidites are shortened by short-wavelength folds and imbricated thrusts, detached within the Tertiary Marly Group. In the deeper part of the sections, the uppermost part of the basement is stepped due to the presence of major thrusts, as also confirmed by 2D and 3D gravimetric modelling (Mancinelli et al., 2019, 2020). These steps are located beneath the main topographic/structural culminations of the region, e.g. Monti Sibillini and Montagna dei Fiori. A similar structural style, with stacked carbonate units above a stepped basement, was also used by Fantoni and Franciosi (2010); see their Fig. 8), who drew a set of regional-scale geological sections through the external part of the whole Apennines belt, based on a vast data-set of industrial seismic profiles and deep boreholes.

As we already know from the description of the surface geology, the compressional structures are systematically cross-cut and displaced by the later (i.e. Quaternary) normal faults, responsible for the seismic activity of this region, whose position and attitude is very well known at the surface, where they have been mapped in detail by many authors (e.g. Pierantoni et al., 2013; Brozzetti et al., 2019); many are poorly imaged by the available seismic profiles, which yield only few insights into their extrapolation to depth (see e.g. Figs. 5 to 7).

4.1. Subsurface geology and seismicity distribution

Along the five sections (Fig. 8) we have plotted the 2016–17 seismicity, derived from the data-set published by Michele et al. (2020), consisting of all the $M_L > 1.5$ earthquakes that occurred in the study region between August 2016 and October 2018. These ca. 34,000 events, relocated by applying double difference techniques (Waldhauser and Ellsworth, 2000), have a formal error smaller than 300 m in both horizontal and vertical direction, and can therefore be certainly compared to the geological features. As the 24th of August (Amatrice) event was the first shock of the sequence, it was recorded only at the permanent stations of the national network; the temporary stations, densifying the network, were added only in the coming days. Thus, this main event shows the largest uncertainties in the hypocentre parameters (Michele et al., 2020). For this reason, only for this major earthquake, we adopted a more recent solution, proposed by Waldhauser et al., 2020, locating the mainshock at about 6.5 km depth.

For each section, we selected the seismicity, occurring in a strip 6 km wide, ± 3 km from each side of the traces reported in Fig. 1a; for the S05 section, a wider strip (8 km) was selected, in order to include all the four $M_W > 5$ events that occurred in January 2018 (see map in Fig. 1). We also plotted the position and focal mechanism solutions of the main shocks (with $Mw > 5.0$). While comparing the seismicity distribution with the imaged geological structures (and evaluating reciprocal fit or misfit), it is important to keep in mind that the velocity model used for the depth conversion of the seismic profiles is not the same as that used for the localization of the earthquakes' foci, which is a 1-D gradient version of the P- and S-wave velocity model (after Carannante et al., 2013). Thus, we can regard these two sets of data as being completely independent.

In all the cross sections of Fig. 8, the seismicity is distributed within a rock volume about 10 km thick, oriented nearly parallel to the NNW-trending attitude of the main normal fault segments mapped at the surface and dipping about 45° towards WSW. Within this volume, we divide the observed seismicity into four major groups based on location relative to actual or inferred geological structures:

- *Group 1* (Master Fault seismicity, MFs) is a strip, 1 to 2 km thick, grossly aligned along the trajectory of the activated main normal fault hosting the mainshock (e.g. focal mechanisms) and related aftershocks;
- *Group 2* (Hangingwall seismicity, HWs) and *Group 3* (Footwall seismicity, FWs) consist of the events located within the master fault hangingwall and footwall blocks, respectively, whose distribution and/or clustering varies considerably through the different sections; and
- *Group 4* (Basal Fault zone, BFz) consists of the events located along a layer, about 2 km thick, corresponding to the bottom of the observed seismicity, and therefore here identified as a "Basal Fault zone", BFz (the same alignment is termed "Shear Zone, SZ" by Michele et al., 2020). In all the sections, the western part of the BFz is flat or gently east-dipping, whilst its eastern part dips eastward with a steeper trajectory (15° to 25°).

In the following sections, we describe the seismicity distribution, and the characteristics of the four groups along the five geological sections, from N to S (Fig. 8).

Along **Section S01** (Fig. 8b), the overall seismicity is distributed within a volume about 10 km thick, almost symmetrically with compared to the Cupi-Ussita fault, which is also imaged by the MFs alignment. In the western portion of the section, the 1997 aftershocks are aligned along the W-dipping Sellano fault (Chiaraluce et al., 2005), and at a distance of about 10 km from the almost perfectly parallel Cupi-Ussita Fault. Both HWs and FWs are well developed and consist of two shallow groups of earthquakes ($D < 3$ km), about 2 km thick, located in the hangingwall of the MSt. The seismicity of FWs is aligned at the base of the Pizzo Tre Vescovi thrust. The BFz consists of an almost flat, about 1.5 km thick layer of seismicity, whose bottom is located at a depth of about 9 km; towards the east, seismicity is much less abundant and dips eastward, about 20°.

Along **Section 02** (Fig. 8c), the seismicity is distributed asymmetrically with respect to the M. Bove Fault, being more abundant in the footwall block, where it propagates to a distance of about 7 km from the

master fault. MFs dips at a shallower angle compared to the SW-dipping nodal plane of the focal mechanism (46°). FWs contain a major, gently west-dipping, about 2 km thick cluster of seismicity, developed within the Umbria-Marche Unit (U1), i.e. in the hangingwall of the MSt. HWs consists of scarce and sparser seismicity, possibly clustering in correspondence of antithetic and minor synthetic splays of the M. Bove fault. Beneath the activated master fault, the BFz is a dense, gently *E*-dipping cluster, up to 2 km thick, whose bottom is located at a depth of about 8 km and evolves eastward into a relatively steep (about 22°) trajectory.

Along **Section 03** (Fig. 8d), as in the previous section, the seismicity is asymmetrical with respect to the M. Vettore Fault, propagating prevalently in the footwall blocks, at distances up to 10 km from the master fault. Again, the MFs is aligned at a lower angle compared to the SW-dipping nodal plane of the focal mechanism (46°). Within the footwall block, seismicity is clustered at two different depths, being 1–4 and 6–8 km, respectively: the shallower, prominent cluster, resembles the occurrence of conjugate normal faults, affecting the Carbonates and the Evaporites of the Sarnano-Cittareale Unit (U2), at the footwall of the MSt; the deeper seismicity contains a group of minor clusters, mainly hosted in the evaporites of the underlying Acquasanta-Gorzano Unit (U3). HWs consists of scarce, poorly clustered events at a depth of 2–4 km, mainly in the hangingwall of the MSt, and of sparser seismicity, possibly clustering in correspondence of antithetic and minor synthetic splays of the master fault. The pattern of the BFz is quite similar to that of S02, with a dense, gently E-dipping cluster, up to 2 km thick, located at a depth of about 8 km beneath the M. Vettore Fault. The eastern part dips eastward about 20°.

Section 04 (Fig. 8e) crosses the transfer zone between the SE termination of the M. Vettore Fault and the NW termination of the M. Gorzano Fault (see map in Fig. 1a). It is characterised by an extreme scarcity of shallow seismicity. Consequently, the seismicity is almost totally focused along the BFz, consisting of a nearly horizontal and relatively thin western portion, at a depth of 9–9.5 km, propagating eastward into a steeper (20°) segment, reaching a depth of about 12 km. Above the BFz, only sparse seismicity is observed, possibly aligned along the two above-mentioned fault segments.

Along **Section S05** (Fig. 8f), most of the seismicity is clustered along the trajectory of the Campotosto Fault, and defines a pronounced listric geometry, characterised by a much lower dip angle, compared with that imaged by the SW-dipping nodal plane of the focal mechanisms (ca. 46°). The southernmost portion of the Campotosto Fault segment was also reactivated during the late phases of the L'Aquila 2009 sequence, showing the same listric geometry (Chiaraluce, 2012; Lavecchia et al., 2011, 2012; Valoroso et al., 2013). Seismicity here is totally confined within the Carbonates and Evaporites of the deepest tectonic unit (Montagna dei Fiori Unit, U4), not propagating into the overlying Laga turbidites, nor into the uppermost Acquasanta-M. Gorzano Unit (U3). The FWs consists of a single cluster, at a depth of 10–11 km, possibly corresponding to an antithetic normal fault. By contrast, the HWs is represented by sparse events, located at shallower depth (4–6 km) within the Acquasanta-M. Gorzano Unit (U3) and possibly aligned along the trajectory of the Montereale Fault. This is the only section where the BFz is not easily traceable: we can only recognise a deep (11–12 km), dense cluster of seismicity located at the base of the seismogenic normal fault, but only few events mark its possible, eastward and westward, prolongations.

5. Discussion

5.1. Seismicity distribution with depth

The histograms of Fig. 9 offer a comprehensive view of the seismicity distribution with depth, along the 5 cross sections. For each section, two histograms have been devised: those in black show the total number of events observed from August 2016 to January 2018 whilst those in color show events that occurred during the first two days following the mainshock (MW > 5) events intersected by each cross section ("early aftershocks", sensu Improta et al., 2019).

Most histograms (with the exception of that related to section S04) are characterised by a pronounced bimodality. The deeper mode, present in all the sections, corresponds to the BFz and clearly deepens southward (i.e. from S01 to S05) from about 8 km to about 11 km. In the sections crossing the M. Vettore-M. Bove Fault System (S01, S02 and S03), the shallower mode (1–3.5 km deep) include both HWs and FWs, occurring in the uppermost tectonic units, consisting of Carbonates and Evaporites. In the sections crossing the Laga Fault System (S04 and S05),

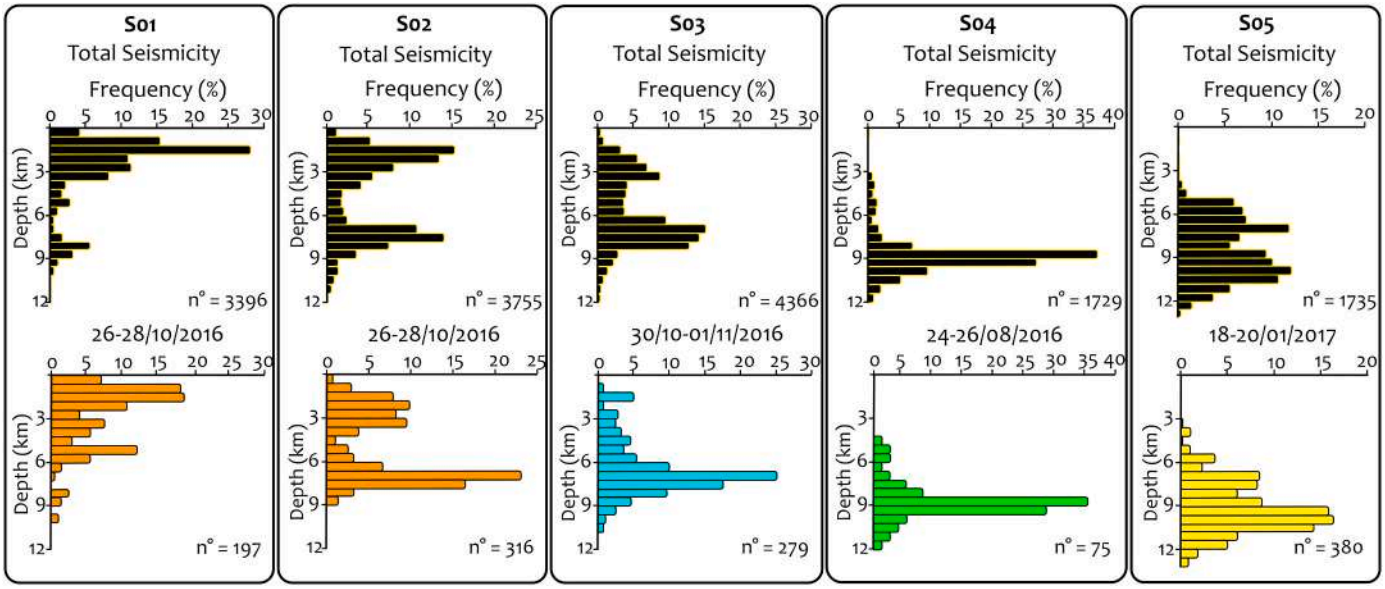

Fig. 9. Seismicity distribution with depth. Frequency histograms showing the number of events registered along the five geological cross sections of Figure 8. The black histograms (above) represent the total seismicity projected along each section, while the color histograms (below) represent the events within the two days following the corresponding mainshocks (early aftershocks EAs, see text for discussion), i.e.: orange (S01 and S02) M_W 5.9 (26/10/2016); light blue (S03) M_W 6.5 (30/10/2016); green (S04) M_W 6.0 (24/08/2016); yellow (S05) M_W 5.5 (18/01/2017). (For interpretation of the references to color in this figure legend, the reader is referred to the web version of this article.)

the absence of this shallow seismicity is related to presence in the uppermost part of these sections of a thick layer of Turbidites (mainly sandstones and marls of the Laga Fm.), where very few earthquakes are generally observed (e.g. Latorre et al., 2016; Barchi and Collettini, 2019; Michele et al., 2020). However, it is worth noting that along our sections S04 and S05, the layer lacking earthquakes is often thicker that the Turbidites layer. Whilst the histogram of section S04 shows just a single mode, corresponding to the BFz, a peculiar distribution characterizes section S05, whose bimodality is due to the abundant seismicity occurring at intermediate depth (5–8 km), in the Carbonates and Evaporites overlying the BFz layer, which along this section reaches its maximum depth (9–12 km).

5.2. Geometry of the seismological faults

The seismicity distribution, in comparison with the geological structures mapped at the surface and extrapolated to depth, along the whole set of five cross-sections of Fig. 8, gives insights into the geometry of the seismogenic master faults active during the 2016–2017 sequence.

First of all, our sections confirm that the position and trajectory of the activated faults, depicted by the seismological data (i.e. MFs), are generally consistent with the position at the surface of the Quaternary normal faults and of the co-seismic ruptures, and with their trajectory at depth, suggested by the available seismic data. Indeed, almost complete consensus exists on the connection between the Quaternary normal faults exposed at the surface and the faults seismically activated at depth ("geological faults" vs. "seismological faults", sensu Chiaraluce et al., 2005; Barchi and Mirabella, 2009, see also Valensise et al., 2016; Bonini et al., 2019). A similar connection has been also observed for the northernmost Colfiorito Fault system, activated by the 1997–98 seismic sequence (Chiaraluce et al., 2005). For the M. Vettore-M. Bove Fault System, this connection was further confirmed by the occurrence of co-seismic surface ruptures along the long-term Quaternary faults (Brozzetti et al., 2019; Civico et al., 2018; Villani et al., 2018, 2018a; Cirillo, 2020). The formation of these surface ruptures was monitored in situ by precise co-seismic GPS measurements (Wilkinson et al., 2017), showing that they are connected to the seismic sources not only in space, but also in time. For the Laga Fault System, even in the absence of clear co-seismic ruptures during the 2016–2017 earthquakes, Holocene reactivation of the Quaternary faults is solidly proven by geomorphological evidence (Cacciuni et al., 1995), and paleo-seismological trenches (Galadini and Galli, 2003; Falcucci et al., 2018).

The correlation between surface geology and seismicity is more problematic, when the second order extensional structures, formed in the hangingwall and/or footwall blocks of the Quaternary master faults, are considered. In many sections (e.g. S02, S03, S04), the rock volume affected by the seismicity is quite asymmetric, being thicker and more abundant, in the footwall block (i.e. FWs) than in the hangingwall block. This contrasts with the observation that most of the co-seismic ruptures, observed at the surface (Distributed deformation, sensu Ferrario and Livio, 2018), as well as most of the Quaternary synthetic and antithetic splays, occur in the hangingwall of the activated master faults (e.g. Pierantoni et al., 2013), which also experienced larger displacements compared to the footwall blocks (Bignami et al., 2019). Similar observations have been also reported for normal fault zones from other regions worldwide, where the damage zones are significantly thicker in the hanging walls compared with the footwalls (Reyer et al., 2012 and references therein).

Moving from the surface and following the fault trajectory at depth, combined geological and seismological data suggest that the dip of the activated faults diminishes, as already observed in the Colfiorito area (Chiaraluce et al., 2005; Barchi and Mirabella, 2009). The major seismogenic normal faults are steeper at the surface (where they crop out dipping 60°–70°, e.g. Pierantoni et al., 2013; Brozzetti et al., 2019) and become gentler at depth, as also suggested by the nodal plane of the focal mechanisms (42°–50°; Scognamiglio et al., 2018), as well as by the alignments of seismicity (i.e. MFs), connecting the mainshocks to the active master faults exposed at the surface, which apparently dip less than 40° (Fig. 8). Unfortunately, the resolution of our seismic data is not good enough to discriminate if the fault dip changes continuously, describing a proper curvilinear (i.e. listric) fault trajectory (as proposed by Ciaccio et al., 2005 for the Gualdo Tadino fault) or if the fault is composed of an alignment of few planar segments with progressively lower dip, as proposed by Chiaraluce (2012) for the southernmost portion of the Campotosto Fault activated during the 2009 L'Aquila sequence. It is important to note that, in most cases, the high-resolution seismological data collected in Central Italy do not support the existence of listric active faults (e.g. Chiaraluce, 2012; Chiaraluce et al., 2017; Michele et al., 2020).

In their deepest part, the seismogenic master faults, imaged by the seismicity distribution (MFs), terminate downward at the intersection with the BFz, which also corresponds to the seismicity cut-off. Beneath the major active normal faults, the depth and attitude of the BFz generally corresponds to the top of the acoustic basement (Porreca et al., 2018; Mancinelli et al., 2019), as recognized in several seismic profiles, and clearly imaged by a prominent reflector in the line NOR02 (Fig. 6c). In the easternmost part of the sections (Figs. 8, 10c), the BFz propagates through the underlying basement, reaching a depth of 11–12 km. The regional *E*-dipping overall geometry of the BFz, forming the seismicity cut-off at depth and containing in its hanging-wall the SW-dipping seismogenic normal faults, is compatible with the hypothesis that this deep fault zone may represent a regional E-dipping detachment, driving the extensional deformation of the region (Lavecchia et al., 2017; Chiarabba et al., 2020).

5.3. Fault segmentation and the role of inherited structures

The overall geological and geophysical evidence illustrated in this paper, clearly indicates that the seismogenic structures activated during the 2016–2017 seismic sequence, consist of a complex, highly-segmented system of thick-skinned, NNW-SSE-trending normal faults. There is clear evidence that fault segmentation, both along strike and down-dip, is affected by the inherited compressional structures in the upper crust.

The most significant features of the activated fault systems are schematically illustrated in Fig. 10, consisting of three different images, aimed to show:

- The traces at the surface of the activated fault system, described in Chapter 2, which along-strike consists of five major segments, NNW to SSE, namely: the Cupi-Ussita Fault (CUF), the M. Bove Fault (BF) and the M. Vettore Fault (VF), forming the M. Vettore-M. Bove Fault System (VBFS); and the M. Gorzano Fault (GF) and the Campotosto Fault (CF), forming the Laga Fault System (LFS) (Fig. 10a);
- The subsurface geometry of the same fault segments, as derived by connecting the trajectory at depth of the faults, imaged along the five geological cross-sections of Fig. 8, with their trace at the surface (Fig. 10b);
- An inclined geological section, dipping WSW 47°, drawn approximately parallel to the envelope of the normal fault planes, showing the geology (i.e. main lithological units and the major thrusts), as viewed looking ENE where it intersects the normal fault system. Along this section, we also projected the seismicity that occurred in both the hanging-wall and foot-wall, for a maximum distance of 2 km from the modelled surface (Fig. 10c).

The inclined geological profile of Fig. 10c offers an immediate, comprehensive view of the relationships between the seismicity distribution and the pre-existing litho-mechanical stratigraphy of the crust (Carminati et al., 2020). The stronger lithological units, such as the Carbonates and Evaporites host the larger part of the seismicity, which is much less abundant in the weaker levels, represented by the Turbidites

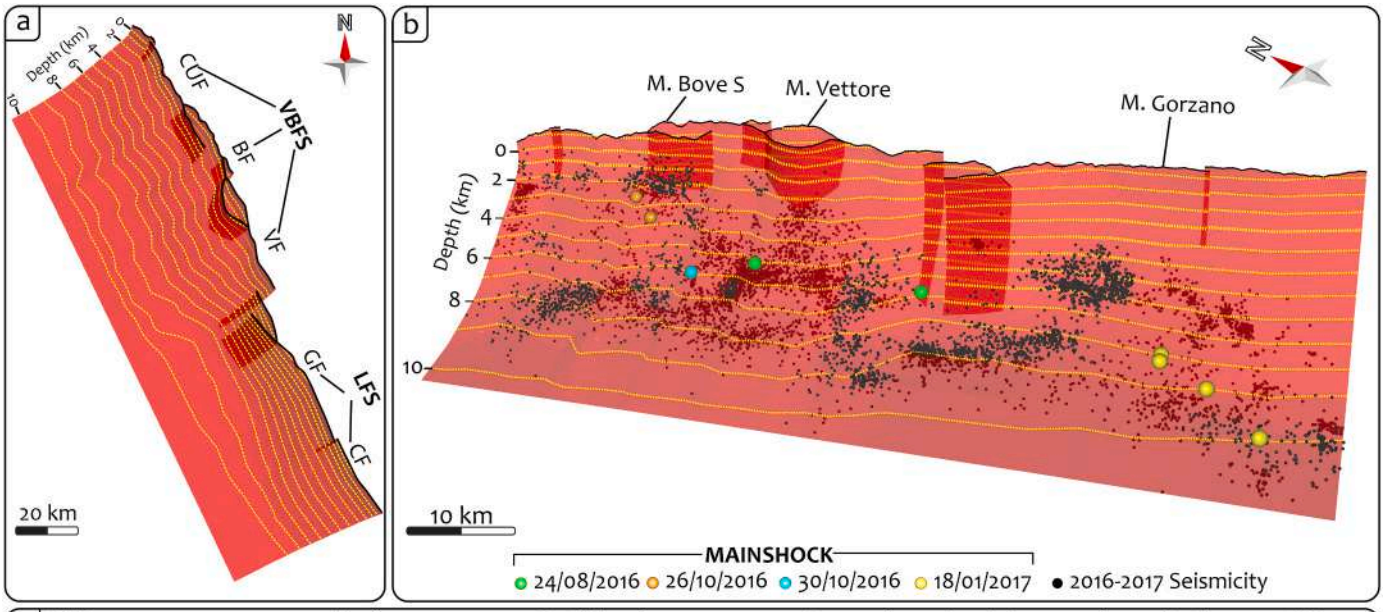

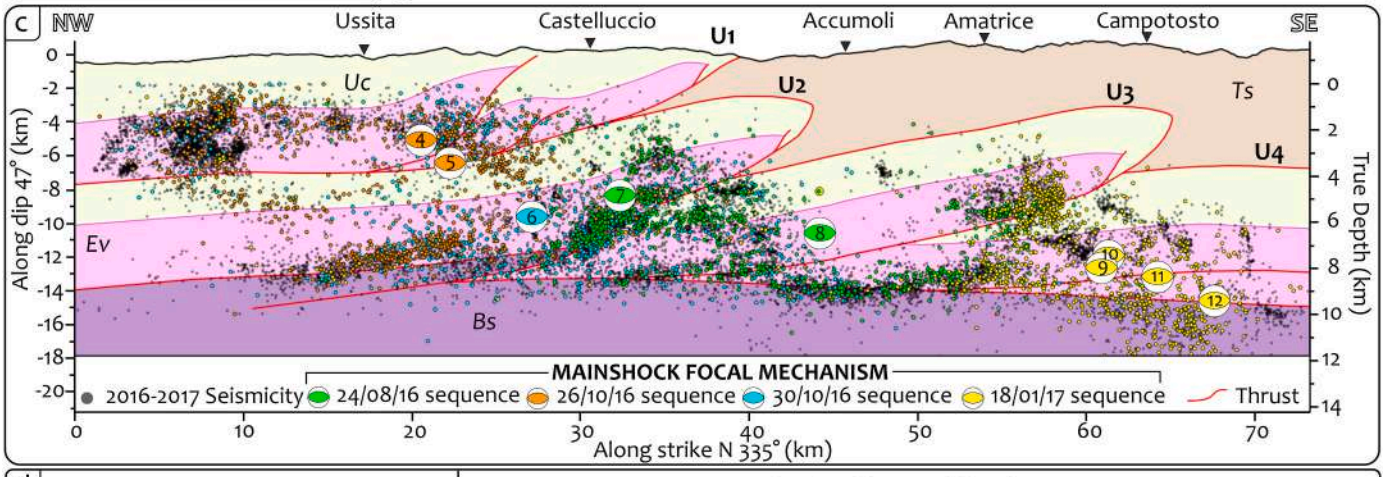

d

Inherited Tectonic Units	Active Normal Faults				
	CUF	BF	VF	GF	CF
Umbria - Marche	26/10/ 2016				
Sarnano - Cittareale		30/10/2016			
Acquasanta - M. Gorzano			24/08/2016		
M . dei Fiori - Montagnone					18/01/ 2017

Fig. 10. Along-strike view of the activated normal fault system. (**a**) 3D view of the fault system showing the relationships between the fault segments exposed at the surface. (**b**) 3D view of the fault system showing the relationships with the instrumental seismicity distribution. Seismicity has been plotted within a total buffer of 1 km from the major normal faults. Seismicity at the hangingwall is shown in black dots while seismicity at the footwall is shown by faded black dots. (**c**) Frontal view of the activated fault system, modelled as a single plane surface, oriented N 335° 47°, showing the tectonic units and lithologies at the fault hanging-wall and the EAs distribution (EAs are coloured following the same legend of Figure 9). EAs has been projected within a total buffer of 4 km; the numbers of the focal mechanisms are referred to Fig. 1b. (**d**) Location of the seismicity associated to the 4 main sub-sequences, in relation with the (active) normal faults and to the (inherited) tectonic units of the study area.

and by the phyllitic, uppermost part of the Basement. At local scale, sub-horizontal seismicity clusters mostly follow the relatively flat attitude of the single, stacked tectonic units, present along the profile. Considering the whole profile, the along-strike seismicity is distributed along a band of variable thickness, reflecting the overall pre-existing SSE-ward deepening of the stacked units.

The complexity of the ruptured system clearly emerges from the history of the seismic sequence, depicted by the seismological data plotted along the profile of Fig. 10c. Here, the early aftershocks, related to the different mainshocks of the sequence, were represented with the same colours, already used for the histograms of Fig. 9; this gives an immediate view of the propagation of the seismic ruptures through time. The sequence, as suggested by Villani et al. (2018b) and Brozzetti et al. (2019), recently summarised by Michele et al. (2020), consists of four

major sub-sequences (Fig. 10c, d), illustrated in the sketches of Fig. 11:

1. The 24th August mainshock (Mw = 6.0) occurred beneath Accumoli village, at the transfer zone between the GF and the VF, with bilateral rupture directivity (Lavecchia et al., 2016; Tinti et al., 2016; Calderoni et al., 2017) (Fig. 11a);
2. The 26th October event (Mw = 5.9) ruptured the northernmost segments of the system, i.e. BF and CUF, with a strong northward directivity (Chiaraluce et al., 2017) (Fig. 11b);
3. The 30th October mainshock (by far the larger one, Mw = 6.5) nucleated at the northern tip line of the VF, where it overlaps with the BF, and propagated bilaterally for about 40 km, rupturing a large part of the system, from the BF to the GF (e.g. Scognamiglio et al., 2018) (Fig. 11c); and
4. The 18th January sequence, including four 5.0 < Mw < 5.5 earthquakes, ruptured the CF (a segment that was previously indicated by only minor seismicity), propagating northward to its northward termination near Amatrice, where it overlaps with the GF (Fig. 11d).

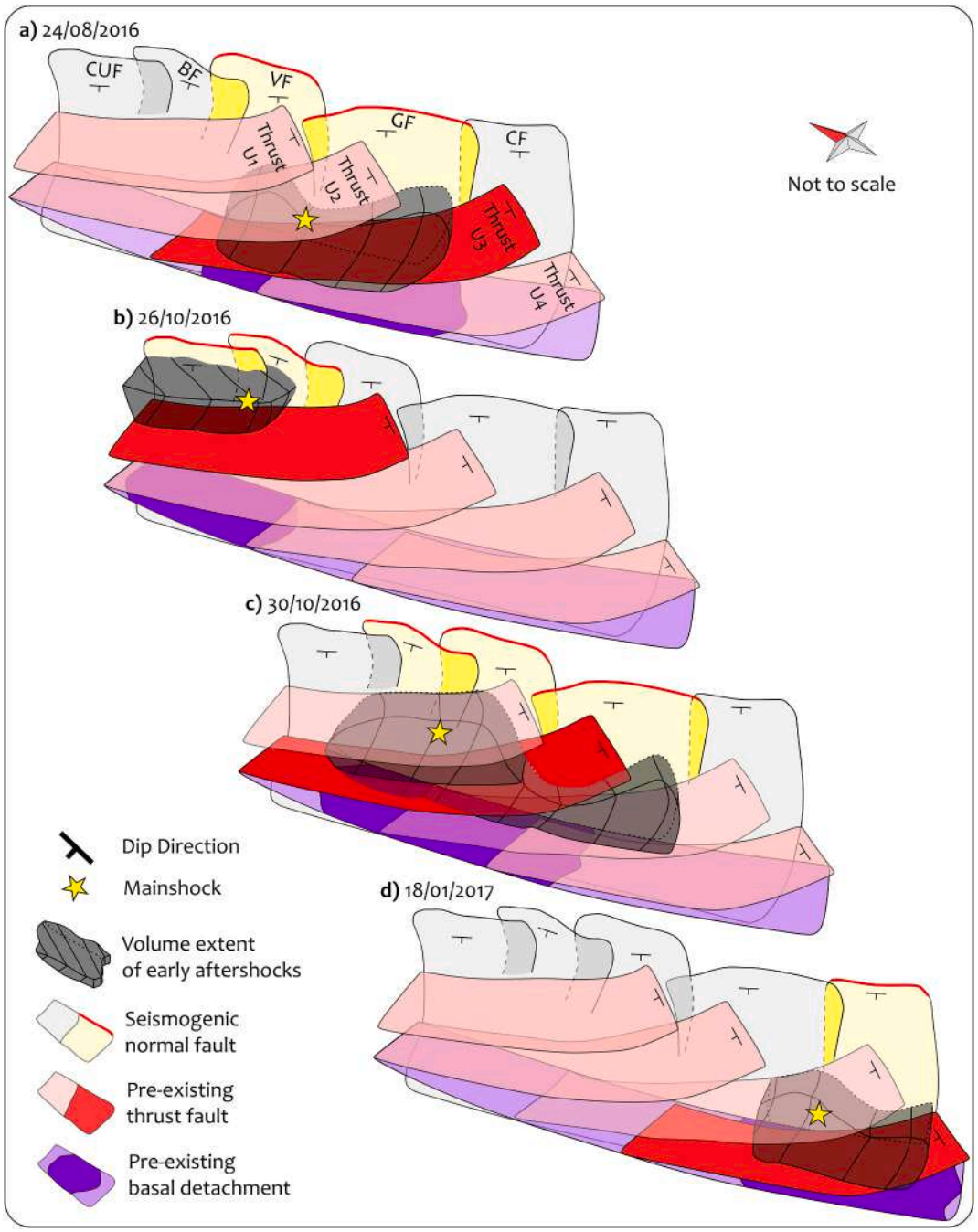

Fig. 11. Synthetic seismotectonic model, illustrating the interactions between the activated normal fault segments, the associated seismicity and the pre-existing thrusts. The four sketches represent the four main stages of the seismic sequence: for each stage, brighter colours characterise the tectonic structures more relevant for the seismogenic process, i.e.: the ruptured normal fault segments, the major thrusts at the base of the seismogenic volume (hosting most of the early aftershocks), the activated portion of the basal detachment. a) 24th August: seismicity is mainly channelled within U3 and U4, activating two central segments (GF and VF); b) 26th October: seismicity is mainly channelled within U1, activating two northern segments (CUF and BF); c) 30th October: seismicity is mainly channelled within U2 and U3, activating the segments VF, BF and GF; d) seismicity is mainly channelled within U4, activating only the southernmost segment CF.

Considering this well-established sequence of events and their spatial distribution with respect to both extensional (i.e. active) and compressional (i.e. inherited) structures, as illustrated along the profile of Fig. 10c and summarised in Fig. 10d and Fig. 11, we can highlight some relevant characteristics of the ruptured fault segments.

The location of the mainshocks indicates that most seismic ruptures nucleated at the endpoint of a fault segment (e.g. Wesnousky, 2006) or in the relay zone of two adjacent segments (e.g. 24th August at the overlap between GF and VF; 26th October at the overlap between BF and CUF; Fig. 11a, b). Unlike the previous seismic sequence in the Apennines (1997–98 Umbria Marche and 2009 L'Aquila), these mainshocks are not located at the bottom of the ruptured faults but at intermediate depths (Michele et al., 2020).

Based on the above described time history of the seismic sequence, in the light of the geological reconstruction shown in Fig. 10c, we suggest that the most important control on the earthquake nucleation is related to the geometrical distribution of the four pre-existing stacked tectonic units (Fig. 10c and Fig. 11). From NNW to SSE, the mainshocks related to the four main sub-sequences occurred within progressively deeper tectonic units, i.e. *Umbria-Marche Unit* (U1, Visso 26th October); *Sarnano-Cittareale Unit* (U2, Norcia 30th October); *Acquasanta-Gorzano Unit* (U3, Accumoli, 24th August); *Montagna dei Fiori-Montagnone Unit* (U4, Campotosto 18th January 2017), as summarised in Fig. 10d and Fig. 11. This also has important implications for the lithological controls on the earthquake nucleation (Carminati et al., 2020) since all the mainshocks occurred at or near the base of the tectonic units, within the Evaporites (Fig. 10c).

We therefore propose a seismotectonic model, schematically illustrated in Fig. 11, where the mainshocks nucleated at the intersection between the tip line of a normal fault segment (dipping about 45°) and a major thrust (dipping less than 20°). In a such model, the tectonic units, consisting of Carbonates and Evaporites, act as "channels" for the lateral propagation of the seismic ruptures, connecting adjacent normal fault segments and driving the rupture propagation across them.

The relay zones between adjacent normal fault segments, in turn, can represent, and often actually act, as effective barriers to the rupture propagation. For example, the relay zone between the BF and VF corresponds to the northern endpoint of the 24th August rupture (Fig. 11a), as well as to the southern endpoint of the 26th October rupture (Fig. 11b). However, the same relay zone had a different behaviour during the 30th October earthquake, which nucleated close to this potential barrier, but propagated into the adjacent fault segments (Fig. 11c). Summarising, the segmentation of the active normal faults seems to affect the location of the mainshocks, which are often nucleated in zones of overlap between adjacent segments.

Our reconstruction also highlights the role played by the inherited, compressional structures in controlling the geometry and segmentation of the active extensional fault system. Previous studies (e.g. Scognamiglio et al., 2018; Improta et al., 2019) postulated the existence at depth of inherited, relatively steep thrust ramps, which were either reactivated as normal/transtensional faults, or acted as barrier, affecting the first order segmentation of the normal fault system. Alternatively, we propose that a major role is played by the shallow-dipping thrusts that delimit the stacked tectonic units, which mostly behave as passive structures, channelizing the seismicity propagation or, in other cases, acting as barriers, as shown in the sketches of Fig. 11.

In addition, the stratigraphy and tectonic setting of the sedimentary cover also affect the along-dip rupture propagation. Even if each earthquake is generated within a specific tectonic unit (Fig. 10d), the related seismicity propagates down-dip through the lower units, down to the BFz, representing the common detachment for the activated fault segments (Fig. 11). The effects of the rupture propagation up-dip are more evident for the segments of the M. Vettore-M. Bove Fault System, affecting the Umbria-Marche Domain, where the seismicity propagates up to the surface forming the well documented co-seismic ruptures; here, the fault trace is also marked by abundant aftershocks. In the segments of the Laga Fault System, the co-seismic effects at the surface are less evident, and we do not observe shallow depth aftershocks.

6. Conclusions

The integrated approach proposed here allows the complexity of the subsurface geology and the distribution of the seismicity to be compared over the whole area involved in the 2016–2017 seismic sequence in Central Italy. The reconstruction of the subsurface geological setting rests on a set of five geological sections, passing through the mainshocks of the sequence, constructed by integrating surface geology and previously unreleased deep seismic data. A set of accurately re-located earthquakes was plotted onto the five geological sections. The along-strike distribution of the seismicity, subdivided into four different subsequences, provides a clear picture of the rupture propagation history and a better comprehension of the involved geological structures (Figs. 10 and 11).

The main insights inferred by our new seismotectonic model are as follows:

- Each seismic rupture starts (nucleates) at the tip line of a major normal fault segment, at a depth where it intersects a pre-existing thrust (i.e. at the base of a tectonic unit);
- Following nucleation, the rupture propagates either along a single fault segment or through multiple adjacent fault segments, following a sub-horizontal "channel" (path) created by the presence of strong rocks (Carbonates and Evaporites) of the involved tectonic unit;
- During the different rupture events, some of the relay zones between adjacent segments may be either open or closed during different episodes of the seismic sequence, mainly depending on the structural depth (i.e. involved structural unit) where the rupture propagates; and
- For each rupture episode (main shock) of the sequence, the total length of the seismogenic fault, and ultimately the earthquake magnitude, depends on the number of involved segments (see Fig. 10d and 11): the larger earthquakes (e.g. Mw = 6.5, 2016/10/30) involved multi-segment ruptures.

These results confirm that the interpretation of seismic profiles gives an improved understanding of the geology at depth, that when integrated with seismological data, allows a far more complete reconstruction of a geomechanical model to account for the evolution of the active fault systems during specified earthquake sequences.

It should always be remembered that a reliable seismotectonic model cannot be based solely on surface geology, since the earthquakes nucleate at depth of several km. In both academic and industrial settings, the accurate reconstruction of the geological structures at such depths requires appropriate geophysical surveys. Among the different geophysical techniques, including both active and passive seismic surveys (e.g. seismic tomography, Chiarabba et al., 2018), seismic reflection data, ideally calibrated with deep boreholes and integrated with other geophysical techniques, are able to support a detailed reconstruction of the fault geometry at depth. These are able to give unique insights into which types of rocks are present at seismogenic depths, a precursor requirement for understanding the mechanics of the active faults and, ultimately, of the earthquakes (e.g. Collettini et al., 2009; Tesei et al., 2014).

The use of 3D seismic reflection surveys is a common, fundamental practice in the industrial sectors. Unfortunately, these kind of data-sets are seldom available for scientific research. In Italy (but also in most other countries) no large programme of geophysical acquisition and/or borehole drilling for scientific purposes has been carried out for many years (e.g. CROP project, Scrocca et al., 2003). As in the case of this study, scientists are therefore forced to re-use vintage industrial surveys, designed and acquired for different aims and targets at the end of the last century.

This is certainly a problem of funding since 3D seismic surveys are very expensive, especially in an on-shore setting. However, the scientific community should make a stronger, more continuous effort for promoting and funding new campaigns of geophysical acquisition, specifically aimed for scientific purposes.

Credit author statement

ME re-processed the geophysical data. MM and LC processed the seismological data. All the authors analysed and interpreted the geological, geophysical and seismological data. MB, FC, CG and SA constructed all the geological cross sections with the MOVE software. FC realized the 3D model of the faults with the MOVE software, and all the figs. MB wrote the manuscript. MB, FC, MM, ME, MP and LC supervised the work and were involved in the review and editing of the manuscript. All authors contributed to the article and approved the submitted version.

Declaration of Competing Interest

We state that this manuscript contains original results, data, ideas and/or interpretations not previously published or under consideration for publication elsewhere (including electronic media and databases).

Acknowledgments

We thankfully acknowledge the Editor R. Carbonell and to the Reviewers F. Brozzetti and R.E. Holdsworth for their precious comments and suggestions, that greatly improved the paper. We are grateful to C. Collettini and R. Arrowsmith for their constructive and stimulating discussions. We also thank Eni S.p.A., that after the occurrence of the seismic crisis in Central Italy, supported this research by kindly providing a large set of unreleased seismic reflection profiles and deep boreholes. The activities of this work were supported by the PRIN (Progetti di Ricerca di Rilevante Interesse Nazionale-Research Projects of Relevant National Interest) research grant funded by the MIUR (Italian Ministry of Education, University and Research) entitled "MUSE 4D: Overtime tectonic, dynamic and rheologic control on destructive multiple seismic events - Special Italian Faults and Earthquakes: from real 4D cases to models" and by the Fondazione Cassa di Risparmio di Perugia (Italy) entitled "Studi geologici di superficie e di sottosuolo sulle faglie sismogeniche dell'Umbria" (Grant BARFCRPG2018, Resp. M.R. Barchi). M. Porreca also acknowledges the support of ASI under the ASI-UniPG agreement 2019-2-HH.0. The database encompassing the geological maps was produced with the software QGIS team; the geological cross sections, the seismic interpretation and the integrated geological sections were constructed with the use of 2D and 3D MOVE 2019 (Petroleum Expert academic licence); conditioning and visualization of seismic reflection profiles were made with dgB Earth Science (OpendTect academic licence).

Appendix A. Supplementary data

Supplementary data to this article can be found online at https://doi.org/10.1016/j.tecto.2021.228797.

References

Anderlini, L., Serpelloni, E., Belardinelli, M.E., 2016. Creep and locking of a low-angle normal fault: Insights from the Altotiberina fault in the Northern Apennines (Italy). Geophys. Res. Lett. 43 (9), 4321–4329.

Bally, A.W., Burbi, L., Cooper, C., Ghelardoni, R., 1986. Balanced cross-sections and seismic reflection profiles across the central Apennines. Mem. Soc. Geol. Ital. 35, 257–310.

Barchi, M.R., 1991. Integration of a seismic profile with surface and subsurface geology in a cross-section through the Umbria-Marche Apennines. Boll. Soc. Geol. Ital. 110, 469–479.

Barchi, M.R., 2010. The Neogene-Quaternary evolution of the northern Apennines: crustal structure, style of deformation and seismicity. J. Virtual Explor. 36 (10) https://doi.org/10.3809/jvirtex.2010.00220.

Barchi, M.R., Collettini, C., 2019. Seismicity of Central Italy in the context of the geological history of the Umbria-Marche Apennines, in Koeberl, C., Bice, D.M. (Eds.), 250 Million Years of Earth History in Central Italy: Celebrating 25 years of the Geological Observatory of Coldigioco. Geol. Soc. Am. Spec. Pap. 542, 175–190.

Barchi, M.R., Mirabella, F., 2009. The 1997-98 Umbria-Marche earthquake sequence: "Geological" vs. "seismological" faults. Tectonophysics 476 (1–2), 170–179.

Barchi, M.R., De Feyter, A., Magnani, M.B., Minelli, G., Pialli, G., Sotera, M., 1998. The structural style of the Umbria-Marche fold and thrust belt. Mem. Soc. Geol. Ital. 52, 557–578.

Barchi, M.R., Lavecchia, G., Galadini, F., Messina, P., Michetti, A.M., Peruzza, L., Pizzi, A., Tondi, E., Vittori, E., 2000. Sintesi delle conoscenze sulle faglie attive in Italia Centrale: parametrizzazione ai fini della caratterizzazione della pericolosità sismica. CNR-GNDT, Projects 5.1.2, 6a2, 5.1.1, Esagrafica, Roma.

Barchi, M.R., Landuzzi, A., Minelli, G., Pialli, G., 2001. Outer Northern apennines. In: Vai, G.B., Martini, I.P. (Eds.), Anatomy of an Orogen: The Apennines and Adjacent Mediterranean Basins Dordrecht. Kluwer Academic Publishers, pp. 215–253.

Beaudoin, N., Labeur, A., Lacombe, O., Koehn, D., Billi, A., Hoareau, G., Boyce, A., John, C.M., Marchegiano, M., Roberts, N.M., Millar, I.L., Claverie, F., Pecheyran, C., Callot, J.-P., 2020. Regional-scale paleofluid system across the Tuscan Nappe – Umbria Marche Arcuate Ridge (northern Apennines) as revealed by mesostructural and isotopic analyses of stylolite-vein networks. Solid Earth 11 (4), 1617–1641. https://doi.org/10.5194/se-11-1617-2020.

Bigi, S., Calamita, F., Cello, G., Centamore, E., Deiana, G., Paltrinieri, W., et al., 1999. Tectonics and sedimentation within a Messinian foredeep in the central Apennines, Italy. J. Pet. Geol. 22 (1), 5–18. https://doi.org/10.1111/j.1747-5457.1999.tb00456.x.

Bigi, S., Casero, P., Ciotoli, G., 2011. Seismic interpretation of the Laga basin; constraints on the structural setting and kinematics of the central Apennines. J. Geol. Soc. 168 (1), 179–190. https://doi.org/10.1144/0016-76492010-084.

Bigi, S., Casero, P., Chiarabba, C., Di Bucci, D., 2013. Contrasting surface active faults and deep seismogenic sources unveiled by the 2009 L'Aquila earthquake sequence (Italy). Terra Nova 25 (1), 21–29. https://doi.org/10.1111/ter.12000.

Bignami, C., Valerio, E., Carminati, E., Doglioni, C., Tizzani, P., Lanari, R., 2019. Volume unbalance on the 2016 Amatrice-Norcia (Central Italy) seismic sequence and insights on normal fault earthquake mechanism. Sci. Rep. 9 (1), 1–13.

Blumetti, A.M., Guerrieri, L., 2007. Fault-generated mountain fronts and the identification of fault segments: implications for seismic hazard assessment. Boll. Soc. Geol. Ital. 126 (2), 307–322.

Blumetti, A.M., Dramis, F., Michetti, A.M., 1993. Fault-generated mountain fronts in the central Apennines (Central Italy): geomorphological features and seismotectonic implications. Earth Surf. Process. Landf. 18 (3), 203–223. https://doi.org/10.1002/esp.3290180304.

Boncio, P., Lavecchia, G., Pace, B., 2004. Defining a model of 3D seismogenic sources for seismic hazard assessment applications: the case of central Apennines (Italy). J. Seismol. 8 (3), 407–425.

Bonini, L., Basili, R., Burrato, P., Cannelli, V., Fracassi, U., Maesano, F.E., et al., 2019. Testing different tectonicmodels for the source of the Mw6.5,30 October 2016, Norcia earthquake (Central Italy): a youthful normal fault, or negative inversion of an old thrust? Tectonics 38, 990–1017. https://doi.org/10.1029/2018TC005185.

Brozzetti, F., Lavecchia, G., 1994. Seismicity and related extensional stress field: the case of the Norcia seismic zone. Annales Tectonicae 8, 38–57.

Brozzetti, F., Boncio, P., Cirillo, D., Ferrarini, F., de Nardis, R., Testa, A., Liberi, F., Lavecchia, G., 2019. High resolution field mapping and analysis of the August - October 2016 coseismic surface faulting (Central Italy Earthquakes): slip distribution, parameterization and comparison with global earthquakes. Tectonics 38, 417–439. https://doi.org/10.1029/2018tc005305.

Cacciuni, A., Centamore, E., Di Stefano, R., Dramis, F., 1995. Evoluzione morfotettonica della conca di Amatrice, Studi Geol. Cam. Vol. Spec. 2, 95–100.

Calamita, F., Deiana, G., 1988. The arcuate shape of the Umbria-Marche-Sabina Apennines (Central Italy). Tectonophysics 146 (1–4), 139–147.

Calamita, F., Pizzi, A., 1994. Recent and active extensional tectonics in the southern Umbro-Marchean Apennines (Central Italy). Mem. Soc. Geol. Ital. 48, 541–548.

Calamita, F., Coltorti, M., Deiana, G., Dramis, F., Pambianchi, G., 1982. Neotectonic evolution and geomorphology of the cascia and Norcia depressions (Umbria-Marche Apennine). Geogr. Fis. Din. Quat. 263–276.

Calamita, F., Pizzi, A., Roscioni, M., 1992. I fasci di faglie recenti ed attive di M. Vettore –M. Bove e di M. Castello – M. Cardosa (appennino Umbro-Marchigiano). Studi Geol. Camerti 81–95. https://doi.org/10.15165/studgeocam-1198.

Calamita, F., Cello, G., Deiana, G., Paltrinieri, W., 1994. Structural styles, chronology rates of deformation, and time-space relationships in the Umbria-Marche thrust system (central Apennines, Italy). Tectonics 13 (4), 873–881.

Calamita, F., Pace, P., Satolli, S., 2012. Coexistence of fault-propagation and fault-bend folding in curve-shaped foreland fold-and-thrust belts: examples from the Northern Apennines (Italy). Terra Nova 24, 396–406. https://doi.org/10.1111/j.1365-3121.2012.01079.x.

Calderoni, G., Rovelli, A., Di Giovambattista, R., 2017. Rupture directivity of the strongest 2016–2017 central Italy earthquakes. J. Geophys. Res. Solid Earth 122, 9118–9131. https://doi.org/10.1002/2017JB014118.

Carannante, S., Monachesi, G., Cattaneo, M., Amato, A., Chiarabba, C., 2013. Deep structure and tectonics of the northern-central Apennines as seen by regional-scale tomography and 3-D located earthquakes. J. Geophys. Res. Solid Earth 118 (10), 5391–5403.

Cardello, L.G., Doglioni, C., 2015. From mesozoic rifting to apennine orogeny: the Gran Sasso range (Italy). Gondwana Res. 27 (4), 1307–1334.
Carminati, E., Bignami, C., Doglioni, C., Smeraglia, L., 2020. Lithological control on multiple surface ruptures during the 2016–2017 Amatrice-Norcia seismic sequence. J. Geodyn. 134, 101676.
Carta Geologica Regionale 1:10000 – Regione Marche, 2014. Regione Marche – P. F. Urbanistica, Paesaggio e Informazioni Territoriali. Retrieved from. http://www.ambiente.marche.it/Territorio/Cartografiaeinformazioniterritoriali/Archiviocartograficoeinformazioniterritoriali/Cartografie/CARTAGEOLOGICAREGIONALE110000.aspx.
Carta Geologica Regionale 1:10000 – Regione Umbria, 2016. Geoportale WebGis Regione Umbria: Direzione Ambiente, Territorio e Infrastrutture Servizio Geologico e Sismico. Retrieved from. http://storicizzati.territorio.regione.umbria.it/Static/GeologiaKmz/Geologia.
Cavinato, G.P., De Celles, P.G., 1999. Extensional basins in the tectonically bimodal central Apennines fold-thrust belt, Italy: response to corner flow above a subducting slab in retrograde motion. Geology 27 (10), 955–958.
Centamore, E., Adamoli, L., Berti, D., Bigi, G., Bigi, S., Casnedi, R., Cantalamessa, R., Fumanti, G., Morelli, F., Micarelli, C., Ridolfi, A., Salvucci, M., 1992. Carta geologica dei bacini della Laga e del Cellino e dei rilievi carbonatici circostanti, in Studi Geologici Camerti, Vol. Università degli Studi, Dipartimento di Scienze della Terra. SELCA, Firenze.
Chiarabba, C., De Gori, P., Cattaneo, M., Spallarossa, D., Segou, M., 2018. Faults geometry and the role of fluids in the 2016–2017 Central Italy seismic sequence. Geophys. Res. Lett. 45, 6963–6971. https://doi.org/10.1029/2018GL077485.
Chiarabba, C., Buttinelli, M., Cattaneo, M., De Gori, P., 2020. Large earthquakes driven by fluid overpressure: the Apennines normal faulting system case. Tectonics 39 (4). https://doi.org/10.1029/2019TC006014 e2019TC006014.
Chiaraluce, L., 2012. Unravelling the complexity of Apenninic extensional fault systems: a review of the 2009 L'Aquila earthquake (central Apennines, Italy). J. Struct. Geol. 42, 2–18. https://doi.org/10.1016/j.jsg.2012.06.007.
Chiaraluce, L., Ellsworth, W.L., Chiarabba, C., Cocco, M., 2003. Imaging the complexity of an active normal fault system: the 1997 Colfiorito (Central Italy) case study. J. Geophys. Res. 108 (B6) https://doi.org/10.1029/2002jb002166.
Chiaraluce, L., Barchi, M.R., Collettini, C., Mirabella, F., Pucci, S., 2005. Connecting seismically active normal faults with Quaternary geological structures in a complex extensional environment: the Colfiorito 1997 case history (Northern Apennines, Italy). Tectonics 24 (1). https://doi.org/10.1029/2004TC001627.
Chiaraluce, L., Di Stefano, R., Tinti, E., Scognamiglio, L., Michele, M., Casarotti, E., Cattaneo, M., De Gori, P., Chiarabba, C., Monachesi, G., Lombardi, A., Valoroso, L., Latorre, D., Marzorati, S., 2017. The 2016 Central Italy seismic sequence: a first look at the mainshocks, aftershocks, and source models. Seismol. Res. Lett. 88 (3), 757–771. https://doi.org/10.1785/0220160221.
Chiarini, E., La Posta, E., Cifelli, F., D'Ambrogi, C., Eulilli, V., Ferri, F., Marino, M., Mattei, M., Puzzilli, L.M., 2014. A multidisciplinary approach to the study of the Montereale Basin (Central Apennines, Italy). Rend. Fis. Acc. Lincei 25, S177–S188.
Chopra, S., Marfurt, K.J., 2007. Seismic Attributes for Prospect Identification and Reservoir Characterization, SEG Geophysical Developments Series No. 11, edited by: Hill, S. J. (series editor and volume editor), ISBN 978–1–56080-141-2 (volume) – ISBN 978–0–931830-41-9 (series), 464 p.
Ciaccio, M.G., Barchi, M.R., Chiarabba, C., Mirabella, F., Stucchi, E., 2005. Seismological, geological and geophysical constraints for the Gualdo Tadino fault, Umbria–Marche Apennines (Central Italy). Tectonophysics 406 (3–4), 233–247. https://doi.org/10.1016/j.tecto.2005.05.027.
Ciarapica, G., 2007. Regional and global changes around the Triassic–Jurassic boundary reflected in the late Norian–Hettangian history of the Apennine basins. Palaeogeogr. Palaeoclimatol. Palaeoecol. 244, 34–51.
Cinti, F.R., Pantosti, D., De Martini, P.M., Pucci, S., Civico, R., Pierdominici, S., Cucci, L., Brunori, C.A., Pinzi, S., Patera, A., 2011. Evidence for surface faulting events along the Paganica fault prior to the 6 April 2009 L'Aquila earthquake (Central Italy). J. Geophys. Res. Solid Earth 116 (B7).
Cinti, F.R., Civico, R., Blumetti, A.M., Chiarini, E., La Posta, E., Pantosti, D., et al., 2018. Evidence for surface faulting earthquakes on the Montereale fault system (Abruzzi Apennines, Central Italy). Tectonics 37, 2758–2776. https://doi.org/10.1029/2017TC00478.
Cirillo, D., 2020. Digital Field Mapping and Drone-Aided Survey for Structural Geological Data Collection and Seismic Hazard Assessment: Case of the 2016 Central Italy Earthquakes. Appl. Sci. 10, 5233. https://doi.org/10.3390/app10155233.
Civico, R., Blumetti, A.M., Chiarini, E., Romana, F., La Posta, C.E., Papasodaro, F., Sapia, V., Baldo, M., Lollino, G., Pantosti, D., 2016. Traces of the active Capitignano and San Giovanni faults (Abruzzi Apennines, Italy). J. Maps 12 (1), 453–459. https://doi.org/10.1080/17445647.2016.1239229.
Civico, R., Pucci, S., Villani, F., Pizzimenti, L., De Martini, P.M., Nappi, R., the Open EMERGEO Working Group, 2018. Surface ruptures following the 30 October 2016 Mw 6.5 Norcia earthquake, Central Italy. J. Maps 14 (2), 151–160. https://doi.org/10.1080/17445647.2018.1441756.
Collettini, C., De Paola, N., Faulkner, D.R., 2009. Insights on the geometry and mechanics of the Umbria–Marche earthquakes (Central Italy) from the integration of field and laboratory data. Tectonophysics 476, 99–109.
Coltorti, M., Farabollini, P., 1995. Quaternary evolution of the "Castelluccio di Norcia" basin (Umbro-Marchean Apennines, Central Italy). Il Quat. 8 (1), 149–166.
Cooper, J.C., Burbi, L., 1986. The geology of the Sibillini Mountains. Mem. Soc. Geol. Ital. 35 (1), 323–347.
Cosentino, D., Cipollari, P., Marsili, P., Scrocca, D., 2010. Geology of the central Apennines: a regional review. J. Virtual Explor. 36 (11).
Cosentino, D., Asti, R., Nocentini, M., Gliozzi, E., Kotsakis, T., Mattei, M., et al., 2017. New insights into the onset and evolution of the central Apennine extensional intermontane basins based on the tectonically active L'Aquila Basin (Central Italy). GSA Bull. 129 (9–10), 1314–1336.
Cresta, S., Monechi, S., Parisi, G., Baldanza, A., Reale, V., 1989. Mesozic-Cenozoic Stratigraphy in the Umbria-Marche Area: Geological Field Trips in the Umbria-Marche Apennines (Italy): Memorie Descrittive Della Carta Geologica d'Italia 39, 185.
D'Agostino, N., Mantenuto, S., D'Anastasio, E., Giuliani, R., Mattone, M., Calcaterra, S., et al., 2011. Evidence for localized active extension in the Central Apennines (Italy) from global positioning system observations. Geology 39 (4), 291–294.
Deschamps, A., Iannaccone, G., Scarpa, R., 1984. The Umbrian earthquake (Italy) of 19 September 1979. Ann. Geophys. 2 (1), 29–36.
Devoti, R., D'Agostino, N., Serpelloni, E., Pietrantonio, G., Riguzzi, F., Avallone, A., Cavaliere, A., Cheloni, D., Cecere, G., d'Ambrosio, C., Franco, L., Selvaggi, G., Metois, M., Esposito, A., Sepe, V., Galvani, A., Anzidei, M., 2017. A combined velocity field of the Mediterranean region. Ann. Geophys. 60 (2), S0215.
Ercoli, M., Pauselli, C., Frigeri, A., Forte, E., Federico, C., 2013. "Geophysical paleoseismology" through high resolution GPR data: A case of shallow faulting imaging in Central Italy. J. Appl. Geophys. 90, 27–40. https://doi.org/10.1016/j.jappgeo.2012.12.001, 2013.
Ercoli, M., Pauselli, C., Frigeri, A., Forte, E., Federico, C., 2014. 3-D GPR data analysis for high-resolution imaging of shallow subsurface faults: the Mt Vettore case study (Central Apennines, Italy). Geophys. J. Int. 198, 609–621. https://doi.org/10.1093/gji/ggu156.
Ercoli, M., Forte, E., Porreca, M., Carbonell, R., Pauselli, C., Minelli, G., Barchi, M.R., 2020. Using seismic attributes in seismotectonic research: an application to the Norcia Mw = 6.5 earthquake (30 October 2016) in Central Italy. Solid Earth 11, 329–348. https://doi.org/10.5194/se-11-329-2020.
Falcucci, E., Gori, S., Bignami, C., Pietrantonio, G., Melini, D., Moro, M., Saroli, M., Galadini, F., 2018. The Campotosto seismic gap in between the 2009 and 2016–2017 seismic sequences of central Italy and the role of inherited lithospheric faults in regional seismotectonic settings. Tectonics 37. https://doi.org/10.1029/2017TC004844.
Fantoni, R., Franciosi, R., 2010. Tectono-sedimentary setting of the Po Plain and Adriatic Foreland. Rend. Fis. Acc. Lincei 21 (1), S197–S209. https://doi.org/10.1007/s12210-010-0102–4.
Ferrario, M.F., Livio, F., 2018. Characterizing the distributed faulting during the 30 October 2016, Central Italy earthquake: a reference for fault displacement hazard assessment. Tectonics 37, 1256–1273. https://doi.org/10.1029/2017TC004935.
Galadini, F., Galli, P., 2003. Paleoseismology of silent faults in the Central Apennines (Italy): the Mt. Vettore and Laga mts. Faults. Ann. Geophys. 46 (5).
Galli, P., Galadini, F., Pantosti, D., 2008. Twenty years of paleoseismology in. Italy: Earth-Sci. Rev. 88 (1–2), 89–117.
Galli, P., Castenetto, S., Peronace, E., 2017. The macroseismic intensity distribution of the 30 October 2016 earthquake in Central Italy (Mw 6.6): Seismotectonic implications. Tectonics 36, 2179–2191. https://doi.org/10.1002/2017TC004583.
Galli, P., Galderisi, A., Peronace, E., Giaccio, B., Hajdas, I., Messina, P., Pileggi, D., Polpetta, F., 2019. The awakening of the dormant mount Vettore fault (2016 Central Italy earthquake, Mw 6.6): paleoseismic clues on its millennial silences. Tectonics 38 (2), 687–705.
Galli, P., Galderisi, A., Marinelli, R., Messina, P., Peronace, E., Polpetta, F., 2020. A reappraisal of the 1599 earthquake in Cascia (Italian Central Apennines): hypothesis on the seismogenic source. Tectonophysics 774, 228287.
Ghisetti, F., Vezzani, L., 1986. Carta geologica del Gruppo M. Siella - M. Camicia – M. Prena – M. Brancastello (Gran Sasso d'Italia, Abruzzo). Società Elaborazioni cartografiche. Firenze, Scale 1, 15,000.
Ghisetti, F., Vezzani, L., 1991. Thrust belt development in the central Apennines (Italy): Northward polarity of thrusting and out-of-sequence deformations in the Gran Sasso Chain. Tectonics 10 (5), 904–919. https://doi.org/10.1029/91TC00902.
Ghisetti, F., Barchi, M.R., Bally, A.W., Moretti, I., Vezzani, L., 1993. Conflicting balanced structural sections across the central Apennines (Italy): problems and implications. In: Spencer, A.M. (Ed.), Generation, Accumulation and Production of Europe's Hydrocarbons III, Special Publication of the European Association of Petroleum Geologists, pp. 219–231. https://www.scec.org/research/ega.
Improta, L., Latorre, D., Margheriti, L., Nardi, A., Marchetti, A., Lombardi, A.M., Castello, B., Villani, F., Ciaccio, M.G., Mele, F.M., Moretti, M., the Bollettino Sismico Italiano Working Group, 2019. Multi-segment rupture of the 2016 Amatrice-Visso-Norcia seismic sequence (Central Italy) constrained by the first high-quality catalog of early aftershocks. Sci. Rep. 9 (1), 6921. https://doi.org/10.1038/s41598-019-43393-2Kmz/Index_kmz.htm.
Koopman, A., 1983. Detachment tectonics in the central Apennines. Italy. Geol. Ultraiectina 30, 1–55.
Latorre, D., Mirabella, F., Chiaraluce, L., Trippetta, F., Lomax, A., 2016. Assessment of earthquake locations in 3-D deterministic velocity models: a case study from the Altotiberina near Fault Observatory (Italy). J. Geophys. Res. Solid Earth 121, 8113–8135. https://doi.org/10.1002/2016JB013170.
Lavecchia, G., 1985. Il sovrascorrimento dei Monti Sibillini: Analisi cinematica e strutturale. Boll. Soc. Geol. Ital. 104, 161–194.
Lavecchia, G., Minelli, G., Pialli, G., 1988. The Umbria-Marches arcuate fold-belt (Italy). Tectonophysics 146, 125–137.
Lavecchia, G., Brozzetti, F., Barchi, M.R., Keller, J., Menichetti, M., 1994. Seismotectonic zoning in east-central Italy deduced from the analysis of the Neogene to present deformations and related stress fields. GSA Bull. 106, 1107–1120.

Lavecchia, G., Boncio, P., Brozzetti, F., Stucchi, M., Leschiutta, I., 2002. New criteria for seismotectonic zoning in Central Italy: Insights from the Umbria-Marche Apennines. Bollettino Società Geologica Italiana. Spec. Pub. 1, 881–890.

Lavecchia, G., Boncio, P., Brozzetti, F., de Nardis, R., di Naccio, D., Ferrarini, F., Pizzi, A., Pomposo, G., 2011. The April 2009 L'Aquila (Central Italy) seismic sequence (Mw 6.3): a preliminary seismotectonic picture. In: Guarnieri, P. (Ed.), Recent Progress on Earthquake Geology. Nova Science Publishers, pp. 1–17.

Lavecchia, G., Ferrarini, F., Brozzetti, F., De Nardis, R., Boncio, P., Chiaraluce, L., 2012. From surface geology to aftershock analysis: Constraints on the geometry of the L'Aquila 2009 seismogenic fault system. IJG 131 (3). https://doi.org/10.3301/IJG.2012.24.

Lavecchia, G., Castaldo, R., de Nardis, R., de Novellis, V., Ferrarini, F., Pepe, S., Brozzetti, F., Solaro, G., Cirillo, D., Bonano, M., Boncio, P., Casu, F., De Luca, C., Lanari, R., Manunta, M., Manzo, M., Pepe, A., Zinno, I., Tizzani, P., 2016. Ground deformation and source geometry of the 24 August 2016 Amatrice earthquake (Central Italy) investigated through analytical and numerical modeling of DInSAR measurements and structural-geological data. Geophys. Res. Lett. 43 (12) https://doi.org/10.1002/2016GL071723, 389–12.

Lavecchia, G., Adinolfi, G.M., de Nardis, R., Ferrarini, F., Cirillo, D., Brozzetti, F., De Matteis, R., Festa, G., Zollo, A., 2017. Multidisciplinary inferences on a newly recognized active east-dipping extensional system in Central Italy. Terra Nova. https://doi.org/10.1111/ter.12251.

Lomax, A., Virieux, J., Volant, P., Berge, C., 2000. Probabilistic earthquake location in 3D and layered models: introduction of a Metropolis-Gibbs method and comparison with linear locations. In: Thurber, C.H., Rabinowitz, N. (Eds.), Advances in Seismic Event Location. Kluwer, pp. 101–134.

Mancinelli, P., Porreca, M., Pauselli, C., Minelli, G., Barchi, M.R., Speranza, F., 2019. Gravity and magnetic modeling of Central Italy: insights into the depth extent of the seismogenic layer. Geochem. Geophys. Geosyst. 20 (4), 2157–2172. https://doi.org/10.1029/2018GC008002.

Mancinelli, P., Pauselli, C., Fournier, D., Fedi, M., Minelli, G., Barchi, M.R., 2020. Three-dimensional gravity local inversion across the area struck by the 2016–2017 seismic events in Central Italy. J. Geophys. Res. Solid Earth 125. https://doi.org/10.1029/2019JB018853 e2019JB018853.

Marfurt, K.J., 2018. Seismic attributes as the framework for data integration throughout the oilfield life cycle. SEG, 508 p.

Martinis, B., Pieri, M., 1964. Alcune notizie sulla formazione evaporitica del Triassico Superiore nell'Italia centrale e meridionale. Mem. Soc. Geol. Ital. 4, 649–678.

Massoli, D., Koyi, H.A., Barchi, M.R., 2006. Structural evolution of a fold and thrust belt generated by multiple décollements: analogue models and natural examples from the northern Apennines (Italy). J. Struct. Geol. 28 (2), 185–199. https://doi.org/10.1016/j.jsg.2005.11.002.

Mazzoli, S., Pierantoni, P.P., Borraccini, F., Paltrinieri, W., Deiana, G., 2005. Geometry, segmentation pattern and displacement variations along a major Apennine thrust zone, Central Italy. J. Struct. Geol. 27, 1940–1953. https://doi.org/10.1016/j.jsg.2005.06.002.

Menichetti, M., Coccioni, R., 2013. Umbria -Marche Apennines geological feld trip. 2013, Livret-Guide des Excursions du Groupe Francais du Cretaceo, hal-01236473.

Michele, M., Di Stefano, R., Chiaraluce, L., Cattaneo, M., De Gori, P., Monachesi, G., Latorre, D., Marzorati, S., Valoroso, L., Ladina, C., Chiarabba, C., Lauciani, V., Fares, M., 2016. The Amatrice 2016 seismic sequence: a preliminary look at the mainshock and aftershocks distribution. Ann. Geophys. 59.

Michele, M., Chiaraluce, L., Di Stefano, R., Waldhauser, F., 2020. Fine-scale structure of the 2016–2017 Central Italy seismic sequence from data recorded at the Italian National Network. J. Geophys. Res. Solid Earth 125. https://doi.org/10.1029/2019JB018440 e2019JB018440.

Mirabella, F., Barchi, M.R., Lupattelli, A., 2008. Seismic reflection data in the Umbria Marche region: Limits and capabilities to unravel the subsurface structure in a seismically active area. Ann. Geophys. 51 (2–3), 383–396. https://doi.org/10.4401/ag-3032.

Mirabella, F., Brozzetti, F., Lupattelli, A., Barchi, M.R., 2011. Tectonic evolution of a low-angle extensional fault system from restored cross sections in the northern Apennines (Italy). Tectonics 30, TC6002. https://doi.org/10.1029/2011TC002890.

Montone, P., Mariucci, M.T., 2020. Constraints on the structure of the shallow crust in Central Italy from geophysical log data. Sci. Rep. 10, 3834. https://doi.org/10.1038/s41598-020-60855-0.

Patacca, E., Scandone, P., Di Luzio, E., Cavinato, G.P., Parotto, M., 2008. Structural architecture of the central Apennines: interpretation of the CROP 11 seismic profile from the Adriatic coast to the orographic divide. Tectonics 27 (3).

Pauselli, C., Barchi, M.R., Federico, C., Magnani, M.B., Minelli, G., 2006. The crustal structure of the northern Apennines (Central Italy): an insight by the CROP03 seismic line. Am. J. Sci. 306 (6), 428–450. https://doi.org/10.2475/06.2006.02.

Pfiffner, O.A., 2017. Thick-Skinned and Thin-Skinned Tectonics: a Global Perspective. Geosciences 7 (3), 71–89. https://doi.org/10.3390/geosciences7030071.

Pierantoni, P.P., Deiana, G., Galdenzi, S., 2013. 2013. Stratigraphic and structural features of the Sibillini Mountains (Umbria–Marche Apennines, Italy). Ital. J. Geosci. 132, 497–520. https://doi.org/10.3301/IJG.2013.08.

Poblet, J., Lisle, R.J., 2011. Kinematic evolution and structural styles of fold-and-thrust belts. Geol. Soc. Lond. Spec. Publ. 349, 1–24. https://doi.org/10.1144/SP349.1.

Pondrelli, S., Salimbeni, S., Ekström, G., Morelli, A., Gasperini, P., Vannucci, G., 2006. The Italian CMT dataset from 1977 to the present. Phys. Earth Planet. Inter. 159, 286–303. https://doi.org/10.1016/j.pepi.2006.07.008.

Porreca, M., Minelli, G., Ercoli, M., Brobia, A., Mancinelli, P., Cruciani, F., Giorgetti, C., Carboni, C., Mirabella, F., Cavinato, G., Cannata, A., Pauselli, C., Barchi, M.R., 2018. 2018. Seismic reflection profiles and subsurface geology of the area interested by the 2016–2017 earthquake sequence (Central Italy). Tectonics 37, 1–22. https://doi.org/10.1002/2017TC004915.

Porreca, M., Fabbrizzi, A., Azzaro, S., Pucci, S., Del Rio, L., Pierantoni, P.P., Giorgetti, C., Roberts, G., Barchi, M.R., 2020. 3D geological reconstruction of the M. Vettore seismogenic fault system (Central Apennines, Italy): Cross-cutting relationship with the M. Sibillini thrust. J. Struct. Geol. 131, 103938. https://doi.org/10.1016/j.jsg.2019.103938, 2020.

Pucci, S., De Martini, P.M., Civico, R., Villani, F., Nappi, R., Ricci, T., Azzaro, R., Brunori, C.A., Caciagli, M., Cinti, F.R., Sapia, V., De Ritis, R., Mazzarini, F., Tarquini, S., Gaudiosi, G., Nave, R., Alessio, G., Smedile, A., Alfonsi, L., Cucci, L., Pantosti, D., 2017. Coseismic ruptures of the 24 August 2016, Mw6.0 Amatrice earthquake (Central Italy). Geophys. Res. Lett. 44, 2138–2147. https://doi.org/10.1002/2016GL071859.

Reyer, D., Bauer, J.F., Philipp, S.L., 2012. Fracture systems in normal fault zones crosscutting sedimentary rocks, Northwest German Basin. J. Struct. Geol. 821 (45), 38–51.

Rovida, A., Locati, M., Camassi, R., Lolli, B., Gasperini, P., 2016. CPTI15, the 2015 version of the parametric catalogue of Italian earthquakes. Istituto Nazionale di Geofisica e Vulcanologia. https://doi.org/10.6092/INGV.IT-CPTI15

Rovida, A., Locati, M., Camassi, R., et al., 2020. The Italian earthquake catalogue CPTI15. Bull. Earthq. Eng. 18, 2953–2984. https://doi.org/10.1007/s10518-020-00818-y.

Sage, L., Mosconi, A., Moretti, I., Riva, E., Roure, F., 1991. Cross section balancing in the Central Apennines: an application of locace (1). AAPG Bull. 75 (4), 832–844.

Salvini, F., Vittori, E., 1982. Analisi strutturale della Linea Olevano-Antrodoco-Posta (Ancona-Anzio auct.): Metodologia di studio delle deformazioni fragili e presentazione del tratto meridionale. Mem. Soc. Geol. Ital. 24, 337–355.

Scisciani, V., Agostini, S., Calamita, F., Pace, P., Cilli, A., Giori, I., Paltrinieri, W., 2014. Positive inversion tectonics in foreland fold-and-thrust belts: a reappraisal of the Umbria–Marche Northern Apennines (Central Italy) by integrating geological and geophysical data. Tectonophysics 637, 218–237.

Scognamiglio, L., Tinti, E., Michelini, A., 2009. Real-time determination of seismic moment tensor for the Italian region. Bull. Seismol. Soc. Am. 99 (4), 2223–2242.

Scognamiglio, L., Tinti, E., Casarotti, E., Pucci, S., Villani, F., Cocco, M., Magnoni, F., Michelini, A., Dreger, D., 2018. Complex fault geometry and rupture dynamics of the Mw 6.5, 2016, October 30th central Italy earthquake. J. Geophys. Res. Solid Earth 123, 2943–2964. https://doi.org/10.1002/2018jb015603.

Scrocca, D., Doglioni, C., Innocenti, F., Manetti, P., Mazzotti, A., Bertelli, L., Burbi, L., D'Offizi, S., 2003. CROP Ateas: seismic reflection profiles of the Italian crust. Mem. Descr. Carta Geol. It. 66, 194.

Stendardi, F., Capotorti, F., Fabbi, S., Ricci, V., Silvestri, S., Bigi, S., 2020. Geological map of the Mt. In: Vettoretto–Capodacqua Area (Central Apennines, Italy) and Cross-Cutting Relationships between Sibillini Mts. https://doi.org/10.3301/GFT.2020.04. Thrust and Mt. Vettore normal faults system. Geological Field Trips and Maps.

Tavarnelli, E., 1997. Structural evolution of a foreland fold-and-thrust belt: the Umbria-Marche Apennines, Italy. J. Struct. Geol. 19, 523–534.

Tesei, T., Collettini, C., Barchi, M.R., Carpenter, B.M., Di Stefano, G., 2014. Heterogeneous strength and fault zone complexity of carbonate-bearing thrusts with possible implications for seismicity. Earth Planet. Sci. Lett. 408, 307–318. https://doi.org/10.1016/j.epsl.2014.10.021.

Testa, A., Boncio, P., Di Donato, M., Mataloni, G., Brozzetti, F., Cirillo, D., 2019. Mapping the geology of the 2016 Central Italy earthquake fault (Mt. Vettore–Mt. Bove fault, Sibillini Mts.): Geological details on the Cupi–Ussita and Mt. Bove–Mt. Porche segments and overall pattern of coseismic surface faulting. Geol. Field Trips Maps 11 (2.1), 1–13. https://doi.org/10.3301/GFT.2019.03.

Tinti, E., Scognamiglio, L., Michelini, A., Cocco, M., 2016. Slip heterogeneity and directivity of the ML 6.0, 2016, Amatrice earthquake estimated with rapid finite-fault inversion. Geophys. Res. Lett. 43 (10), 745–10,752. https://doi.org/10.1002/2016GL071263.

Valensise, G., Pantosti, D., 2001. The investigation of potential earthquake sources in peninsular Italy: a review. J. Seismol. 5, 287–306.

Valensise, G., Vannoli, P., Basili, R., Bonini, L., Burrato, P., Carafa, M.M.C., Fracassi, U., Kastelic, V., Maesano, F.E., Tiberti, M.M., Tarabusi, G., 2016. Fossil landscapes and youthful seismogenic sources in the central Apennines: excerpts from the 24 August 2016, Amatrice earthquake and seismic hazard implications. Ann. Geophys. 59, 1–10. https://doi.org/10.4401/ag-7215.

Valoroso, L., Chiaraluce, L., Piccinini, D., Di Stefano, R., Schaff, D., Waldhauser, F., 2013. Radiography of a normal fault system by 64,000 high-precision earthquake locations: the 2009 L'Aquila (Central Italy) case study. J. Geophys. Res. 118 (3), 1156–1176.

ViDEPI Project. (2009-2021) - visibility of petroleum exploration data in Italy, Ministry for Economic Development DGRME, Italian Geological Society, Assomineraria. https://www.videpi.com/videpi/videpi.asp (accessed April 2020).

Vignaroli, G., Mancini, M., Bucci, F., Cardinali, M., Cavinato, G.P., Moscatelli, M., Putignano, M.L., Sirianni, P., Santangelo, M., Ardizzone, F., Cosentino, G., Di Salvo, C., Fiorucci, F., Gaudiosi, I., Giallini, S., Messina, P., Peronace, E., Polpetta, F., Reichenbach, P., Scionti, V., Simionato, M., Stigliano, F., 2019. Geology of the central part of the Amatrice Basin Central Apennines, Italy. J. Maps 15 (2), 193–202. https://doi.org/10.1080/17445647.2019.1570877.

Villani, F., Pucci, S., Civico, R., De Martini, P.M., Cinti, F.R., Pantosti, D., 2018. Surface faulting of the 30 October 2016 Mw 6.5 Central Italy earthquake: detailed analysis of a complex coseismic rupture. Tectonics 37, 3378–3410. https://doi.org/10.1029/2018TC005175.

Villani, F., Civico, R., Pucci, S., Pizzimenti, L., Nappi, R., De Martini, P.M., the Open EMERGEO Working Group, 2018a. A database of the coseismic effects following the 30 October 2016 Norcia earthquake in Central Italy. Sci. Data 5, 180049.

Villani, F., Sapia, V., Baccheschi, P., Civico, R., Di Giulio, G., Vassallo, M., Marchetti, M., Pantosti, D., 2019. Geometry and structure of a fault bounded extensional basin by integrating geophysical surveys and seismic anisotropy across the 30 October 2016 Mw 6.5 earthquake fault (Central Italy): the Pian Grande di Castelluccio basin. Tectonics 38, 26–48. https://doi.org/10.1029/2018TC005205.

Waldhauser, F., Ellsworth, W.L., 2000. A double-difference earthquake location algorithm: Method and application to the northern Hayward Fault, California. Bull. Seismol. Soc. Am. 90, 1353–1368. https://doi.org/10.1785/0120000006.

Waldhauser, F., Michele, M., Chiaraluce, L., Di Stefano, R., Schaff, D.P., Ellsworth, W.L., Tan, Y.J., Beroza, G.C., Meier, M., De Gori, P., Chiarabba, C., 2020. Illuminating the complex fault zone structure of the 2016-2017 Amatrice, Central Italy, earthquake sequence with a high-resolution, high-density earthquake catalog. AGU Fall Meeting 2020 (abstract).

Wesnousky, S.G., 2006. Predicting the endpoints of earthquake ruptures. Nature 444 (7117), 358–360.

Wilkinson, M.W., McCaffrey, K.J.W., Jones, R.R., Roberts, G.P., Holdsworth, R.E., Gregory, L.C., et al., 2017. Near-field fault slip of the 2016 Vettore Mw 6.6 earthquake (Central Italy) measured using low-cost GNSS. Sci. Rep. 7 (1), 4612. https://doi.org/10.1038/s41598-017-04917-w.